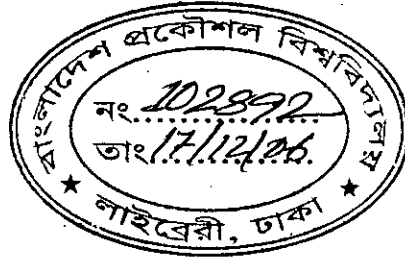


Performance Analysis of a Subcarrier Multiplexed WDM Transmission System in Presence of Fiber Nonlinear Effects

by

Md. Saifuddin Faruk

A Thesis submitted for partial fulfillment of the requirements for the degree of
MASTER OF SCIENCE IN ELECTRICAL & ELECTRONIC ENGINEERING



DEPARTMENT OF ELECTRICAL & ELECTRONIC ENGINEERING
BANGLADESH UNIVERSITY OF ENGINEERING AND TECHNOLOGY

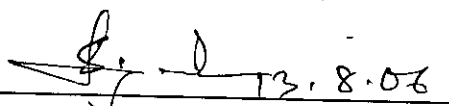
Dhaka-1000 , Bangladesh

August, 2006.



The thesis entitled “**Performance Analysis of a Subcarrier Multiplexed WDM Transmission System in Presence of Fiber Nonlinear Effects**” submitted by Md. Saifuddin Faruk, Roll No: 040406224P. Session: April, 2004 has been accepted as satisfactory in partial fulfillment of the requirement for the degree of **Master of Science in Electrical and Electronic Engineering** on 13 August, 2006

BOARD OF EXAMINERS


13.8.06

Dr. Satya Prasad Majumder

Professor & Head

Department of Electrical & Electronic Engineering

BUET, Dhaka-1000.

Chairman
&
Ex-officio



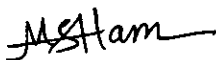
Dr. P. K. Saha

Professor

Department of Electrical & Electronic Engineering

BUET, Dhaka-1000.

Member



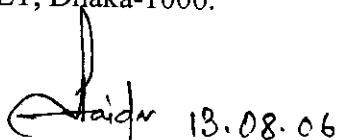
Dr. Md. Shah Alam

Associate Professor

Department of Electrical & Electronic Engineering

BUET, Dhaka-1000.

Member


13.08.06

Wg Cdr Dr. Md. Hossam – e – Haider

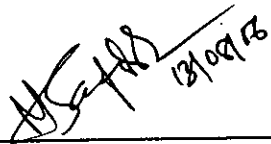
Department of EECE

MIST, Mirpur Cantonment, Dhaka

Member
(External)

CANDIDATE'S DECLARATION

It is hereby declared that this thesis or any part of it has not been submitted elsewhere for the award of any degree or diploma.

 13/09/18

Md. Saifuddin Faruk

CONTENTS

Title page	i	
Board of examiners	ii	
Candidate's declaration	iii	
Contents	iv	
List of figures	vi	
List of abbreviation	x	
Acknowledgement	xi	
Abstract	xii	
Chapter– 1: Introduction		
1.1	Introduction	1
1.2	Fiber Nonlinear Effects in SCM-WDM	3
1.3.1	Stimulated Raman Scattering	3
1.3.2	Cross phase modulation	4
1.3.3	Four wave mixing	4
1.4	Thesis Objectives and Motivation	5
1.5	Organization of the thesis	5
Chapter– 2: Literature Review		
2.1	Subcarrier Multiplexed System	7
2.2	Fiber Nonlinear Effects in SCM-WDM	13
2.3	Four Wave Mixing in WDM System	15
2.4	Summary	19
Chapter– 3: Theoretical Analysis		
3.1	SCM-WDM System Architecture	20
3.2	System description and Operation	22
3.2	SRS Induced Crosstalk	24
3.3	XPM Induced Crosstalk	26
3.4	Constructive & Destructive SRS+XPM Crosstalk Concept	27

3.5	FWM Induced Crosstalk	28
3.5.1	FWM in SCM-WDM System	29
3.6	CNR and BER Calculation	33
3.6.1	Shot noise	33
3.6.2	Thermal noise	34
3.6.3	Relative intensity noise	35
3.6.4	Signal crosstalk noise term	36

Chapter– 4: Results and Discussions

4.1	Effect of XPM Induced Crosstalk	38
4.2	Effect of SRS Induced crosstalk	44
4.3	Combined Effect of SRS and XPM Crosstalk	48
4.4	Effect of FWM Induced Crosstalk	51
4.5	Performance Analysis Using SMF	56
4.6	Performance Analysis Using DSF	61

Chapter – 5: Conclusion

5.1	Conclusion	68
5.2	Recommendations for future work	70
	References	71

List of Figures

Figure		Page
Fig.3.1	Diagram of subcarrier multiplexed lightwave system	20
Fig 3.2	SCM-WDM system architecture	21
Fig 3.3	SRS induced crosstalk	24
Fig.3.4	Demonstration of constructive and destructive concept of SRS+XPM crosstalk	28
Fig.3.5	Power spectrum in fiber input power	30
Fig. 4.1	XPM crosstalk level in three λ channels with varying fiber link length for $\Delta\lambda=1$ nm, $f = 1$ GHz	38
Fig.4.2	XPM crosstalk with varying link length for DSF and SMF	39
Fig.4.3	XPM induced crosstalk with varying link length for different wavelength channel spacing.	40
Fig.4.4	XPM induced crosstalk in central channel vs channel spacing for $L = 25$ km, $f=1$ GHz and $P_{in} = 10$ dBm	40
Fig.4.5	XPM induced crosstalk in central channel with varying link length for different modulation frequency for $\Delta\lambda = 1$ nm and $P_{in} = 10$ dBm	41
Fig.4.6	XPM induced crosstalk in central channel with varying modulation frequency for different fiber link length for $\Delta\lambda = 1$ nm and $P_{in}= 10$ dBm.	42
Fig.4.7	XPM induced crosstalk in different channel with varying optical power per λ channel for $\Delta\lambda = 1$ nm, $L = 25$ km and $f = 1$ GHz.	42
Fig.4.8	XPM crosstalk level in central channel with varying number of WDM channel for $L = 25$, $\Delta\lambda=1$ nm, $P_{in} = 10$ dBm and $f= 1$ GHz	43
Fig.4.9	SRS induced crosstalk in λ_3 channel with varying link length at different modulation frequency for $\Delta\lambda = 1$ nm and $P_{in}=10$ dBm	44
Fig.4.10	SRS induced crosstalk in λ_3 channel with varying modulation frequency for $L= 25$ km, $\Delta\lambda = 1$ nm and $P_{in}=10$ dBm	45

Fig.4.11	SRS induced crosstalk in λ_3 channel with varying modulation frequency at different channel spacing for $L=25$ km, and $P_{in}=10$ dBm	45
Fig.4.12	SRS induced crosstalk in λ_3 channel with varying link length at different channel spacing for $f=0.4$ GHz, and $P_{in}=10$ dBm	46
Fig.4.13	SRS induced crosstalk in λ_3 channel with varying optical launch power per WDM channel $L=25$ km, $\Delta\lambda=1$ nm, $f=1.0$ GHz, and $P_{in}=10$ dBm	47
Fig.4.14	SRS crosstalk level in central channel with varying number of WDM channel for $L=25$, $\Delta\lambda=1$ nm, $P_{in}=10$ dBm and $f=1$ GHz	48
Fig.4.15	Combined crosstalk due to SRS & XPM in three different channels with varying link length for $P_{in}=10$ dBm, $f=0.5$ GHz and $\Delta\lambda=3$ nm.	49
Fig.4.16	Combined crosstalk due to SRS & XPM in three different channels with varying link length for $P_{in}=10$ dBm, $f=0.5$ GHz and $\Delta\lambda=1$ nm.	50
Fig.4.17	Combined crosstalk due to SRS & XPM in three different channels with varying link length for $P_{in}=10$ dBm, $f=1.0$ GHz and $\Delta\lambda=1$ nm.	50
Fig.4.18	FWM efficiency vs wavelength channel spacing for DSF and SMF for $L=25$ km.	52
Fig.4.19	FWM induced crosstalk with varying link length for $M=3$, $N=50$, $P_{in}=0$ dBm and $\Delta\lambda=0.5$ nm.	52
Fig.4.20	FWM induced crosstalk vs number of subcarriers per WDM channel for different number of wavelength channel for $P_{in}=0$ dBm, $\Delta\lambda=0.5$ nm and $L=25$ km.	53
Fig.4.21	FWM induced crosstalk vs number of subcarriers per WDM channel for different number of wavelength channel for $P_{in}=0$ dBm, $M=3$ and $L=25$ km.	54
Fig.4.22	FWM crosstalk with varying optical power per WDM channel for $\Delta\lambda=0.5$ nm, $L=25$, $M=3$, $N=50$.	55

Fig.4.23	BER as a function of optical input power per channel for different channel spacing at bit rate =10 Gb/s, receiver sensitivity = -14dBm, M=3, N=50, $\Delta\lambda=1$ nm.	56
Fig.4.24	Maximum allowable optical input power at BER of 10^{-9} with varying fiber link length at bit rate =10 Gb/s, M=3, N=50, $\Delta\lambda=1.0$ nm & receiver sensitivity= -14 dBm.	57
Fig.4.25	BER as a function of optical input power per channel for different channel spacing at bit rate =10 Gb/s, receiver sensitivity = -14 dBm, M=3, and L=25km.	58
Fig.4.26	Maximum allowable optical input power at BER of 10^{-9} with varying channel spacing at bit rate =10 Gb/s, M=3, N=50, L=25km and receiver sensitivity= -14 dBm.	58
Fig. 4.27	BER as a function of optical input power per channel for different modulation frequency at for $\Delta\lambda=1.0$, receiver sen. = -14dBm, M=3, and L=25km.	59
Fig. 4.28	Fig.4.28: Maximum allowable optical input power at BER of 10^{-9} with varying modulation frequency for L=25 km, M=3, N=50, $\Delta\lambda=1.0$ nm & Rx. sen.= -14 dBm.	60
Fig.4.29	CNR of a RF channel with varying received power for different values of input power at bit rate 10 Gb/s, L=25 km, $\Delta\lambda=0.8$ nm, M=3, N=50.	61
Fig.4.30	BER of a RF channel with varying received power for different values of input power at bit rate 10 Gb/s, L=25 km, $\Delta\lambda=0.8$ nm, M=3, N=50.	62
Fig.4.31	BER as a function of optical input power per channel for different link length at bit rate =10Gb/s, M=3, N=50, $\Delta\lambda=0.5$ nm and receiver sensitivity= -14 dBm.	63
Fig.4.32	Maximum allowable optical input power at BER of 10^{-9} with varying fibre link length for bit rate =10Gb/s, M=3, N=50, $\Delta\lambda=0.5$ nm & receiver sensitivity= -14 dBm.	64
Fig.4.33	BER as a function of optical input power per channel for different number of WDM channel for Bit rate =10Gb/s, receiver sen. = -14dBm, N=50, $\Delta\lambda=0.5$ nm, and L=25km.	64

- Fig.4.34 Maximum allowable optical input power at BER of 10^{-9} with varying number of WDM channel for Bit rate =10Gb/s, N=50, $\Delta\lambda=0.5$ nm, L=25km and receiver sensitivity= -14 dBm. 65
- Fig.4.35 BER as a function of optical input power per channel for different channel spacing at bit rate =10 Gb/s, receiver sensitivity = -14dBm, M=3, N=50 and L=25 km. 66
- Fig.4.36 Maximum allowable optical input power at BER of 10^{-9} with varying channel spacing for Bit rate =10 Gb/s, M=3, N=50, L=25km and receiver sensitivity= -14 dBm. 67

List of Abbreviations

<i>AM-VSB</i>	Amplitude Modulation Vestigial Sideband
<i>BER</i>	Bit Error Rate
<i>CATV</i>	Cable Television
<i>VCO</i>	Voltage controlled Oscillator
<i>CNR</i>	Carrier-Noise-Ratio
<i>CPFSK</i>	Continuous Phase Frequency Shift Keying
<i>CSO</i>	Composite Second Order
<i>CTB</i>	Composite Triple Bit
<i>DFB</i>	Distributed Feedback
<i>DSF</i>	Dispersion Shifted Fiber
<i>DWDM</i>	Dense Wavelength Division multiplexing
<i>FDMA</i>	Frequency Division Multiple Access
<i>FSK</i>	Frequency shift keying
<i>FWM</i>	Four Wave Mixing
<i>GVD</i>	Group Velocity Dispersion
<i>HDTV</i>	High Definition Television
<i>IM/DD</i>	Intensity Modulation/ Direct Detection
<i>ISDN</i>	Integrated Services Digital Network
<i>ISI</i>	Intersymbol Interference
<i>MSK</i>	Minimum Shift Keying
<i>PMD</i>	Polarization Mode Dispersion
<i>PSD</i>	Power Spectral Density
<i>QPSK</i>	Quardature Phase Shift Keying
<i>RF</i>	Radio Frequency
<i>RIN</i>	Relative Intensity Noise
<i>SBS</i>	Stimulated Brillouin Scattering
<i>SCM</i>	Subcarrier Multiplexing
<i>SMF</i>	Single Mode Fiber
<i>SNR</i>	Signal – Noise – Ratio
<i>SRS</i>	Stimulated Raman Scattering
<i>SSB</i>	Single Side Band
<i>TDM</i>	Time Division Multiplexing
<i>WDM</i>	Wavelength Division Multiplexing
<i>XPM</i>	Cross Phase Modulation

ACKNOWLEDGEMENT

The author would like to express his deep gratitude and indebtedness to his supervisor **Dr. Satya Prasad Majumder**, Professor & Head, Department of Electrical and Electronic Engineering, Bangladesh University of Engineering and Technology (BUET), for his continuous inspirations, constructive criticism, guidance, remarkable advice and invaluable supports during this research. Without his whole-hearted supervision, this work would not have been possible.

The author also pays his profound gratitude to his parents, close relatives and friends for their inspiration towards the completion of this work.

The author feels grateful to all of his colleagues and friends, especially to Raju, Shazzat, and Nadim for their invaluable supports throughout this research work.

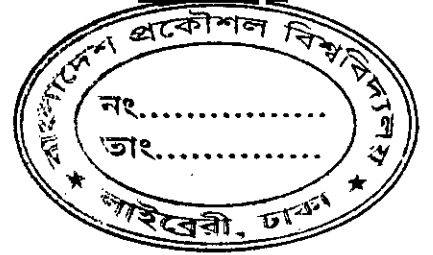
The author is also indebted to librarian and all staffs of the Department of Electrical and Electronic Engineering, BUET, for their cordial help and assistance.

Finally, the author expresses his gratefulness to DUET authority for allowing him to complete this research program granting him leave and necessary permissions.

ABSTRACT

A theoretical analysis for crosstalk level in a subcarrier multiplexed WDM (SCM-WDM) transmission system is presented. Crosstalk due to fiber nonlinear effect is considered as Stimulated Raman Scattering (SRS), Cross Phase Modulation (XPM) and Four Wave mixing (FWM). Analysis is carried out to find the expression for the electric field due to signal and crosstalk at the output of the fiber considering an SCM-WDM signal at the fiber input including the effect of fiber nonlinear effect in a single mode fiber. The type of subcarrier modulation is considered as minimum shift keying (MSK) with optical intensity modulation for the WDM signal. The analysis includes the effect of crosstalk for a direct detection receiver with coherent demodulation of the subcarrier modulated signals. The expression for the carrier power to noise plus crosstalk power ratio and the expression for BER are derived.

Performance results are evaluated for a given fiber length and number of WDM wavelengths for standard Single mode fiber as well as Dispersion shifted fiber at bit rates of 10 Gb/s or more. Optical system optimizing parameters such as optimum input transmitter power, channel separation of wavelength channel, number of WDM channels is evaluated for a BER of 10^{-9} .



CHAPTER-1

INTRODUCTION

1.1 INTRODUCTION

Microwave subcarrier multiplexing (SCM) is an important new approach to design of lightwave system for broad band distribution such as for cable television (CATV) distribution, backbones of wireless network and antenna remoting [1] – [10]. A major objective of the telecommunication industry is to bring low cost broad-band services to the subscriber using optical fibers. To justify the cost of an optical fiber subscriber network it is generally agreed that in addition to the voice and data, video services must be provided. They must also provide maintain a high degree of flexibility and upgradeability so that they can evolve in step with an ever increasing consumer demand for broadband services. In last few years many new ideas has been proposed to meet the increasing demand such as the use of passive optical splitting, high density wavelength division multiplexing, multichannel coherent system, subcarrier multiplexing (SCM) and WDM in conjunction with SCM (SCM-WDM) [3], [24-28].

The attractive features of SCM system are:

1. SCM networks can take the advantage of full range of existing electronic techniques, including analog and digital modulation, as well as microwave and base band signaling.
2. Another attractive feature of SCM in optical communication systems is to provide a way exploit the multigigahertz bandwidth potential of single mode fiber and lightwave components commercially available.
3. SCM system can evolve in step with expected changes in video technology such as high definition television (HDTV), new digital compression techniques etc.
4. Because individual channels are independent, SCM system has great flexibility in allocating bandwidth and thus can readily adapt to rapidly changes of consumer demand.
5. SCM system has further striking feature that it do not exclude simultaneously transmission of conventional base band signal with the same laser, fiber and detector.

Although relatively straightforward to implement using available components, SCM does exhibit some disadvantages, most important of which is associated with source nonlinearities [3]-[6]. Distortion caused by this phenomenon can be particularly noticeable when several subcarriers are transmitted from a single optical source. Moreover, SCM systems, which are expected to employ AM-VSB modulation, must operate at high frequency, often in gigahertz range. In addition for digital system SCM requires more bandwidth per channel than time division multiplexing (TDM).

The combination of Wavelength division multiplexing (WDM) and SCM (SCM-WDM) provides the potential of designing broadband passive optical networks capable of providing integrated services such as audio, video, data etc. to a large number of subscribers. In this scheme multiple optical carriers are launched the same optical fiber through the WDM technique. Each optical carrier carries multiple SCM channels using several microwave subcarriers. One can mix analog and digital signals using different subcarriers or different optical carriers. Such networks are very flexible and easily upgradeable. The main advantage of SCM/WDM system is that the network can serve NM users, where N is the number of microwave subcarriers and M is the number of optical wavelengths. The optical wavelength can be relatively far apart (coarse WDM) for reducing the cost of terminal equipment or Dense WDM (DWDM) for provide a large number of users.

But when wavelengths carrying SCM signals propagates in a fiber, fiber nonlinearities can lead to crosstalk between subcarriers of different wavelengths. In dispersive fiber (such as single mode fiber, SMF) the dominant fiber nonlinearities that causes crosstalk are stimulated Raman scattering (SRS) and cross phase modulation (XPM). To reduce these effects low dispersive fiber (such as dispersion shifted fiber, DSF) can be used but then another fiber nonlinear effect takes place namely four wave mixing (FWM). Though SRS and XPM have been analyzed in some literatures [22-29], effect of FWM is still to be reported. In this thesis performance of a SCM-WDM system is analyzed considering all these nonlinear effects.

1.2 FIBER NONLINEAR EFFECTS IN SCM-WDM

In optics, the terms *linear* and *nonlinear* mean 'power independent' and 'power dependent' phenomena respectively. Due to nonlinear behavior of fiber, the refractive index of the fiber can be written as $n = n_1 + n_2 I$; where n_1 and n_2 are linear and nonlinear refractive index respectively and I is the optical field intensity. This phenomenon is known as Kerr effect.

As mentioned earlier fiber nonlinear effects can be attributed to SRS, XPM and FWM in an SCM-WDM system.

1.2.1 Stimulated Raman Scattering

Raman Scattering arises from interaction between light and vibration of silica molecules in the fiber. Scattered light can appear in both the forward and backward directions. In a single-channel system the "Raman Threshold" (the power level at which Raman Scattering begins to take effect) is very high. Other effects (such as SBS) limit the signal power to much less than the Raman Threshold in single-channel systems. While Stimulated Raman Scattering is a not an issue in single-channel systems it can be a significant problem in WDM systems. When multiple channels are present, power is transferred from shorter wavelengths to longer ones. This can be a useful effect in that it is possible to build an optical amplifier based on SRS. But in the transmission system it is a source of noise.

Notice that power has been transferred from the shorter wavelength to the longer one (from the higher energy wave to the lower energy one). This has resulted in additive noise at the longer wavelength and subtractive noise at the shorter one. This power transfer is caused by interactions of the light with vibrating molecules. Optical power so transferred is called the "Stokes Wave". Important characteristics of SRS are: The effect of SRS becomes greater as the signals are moved further and further apart (within some limits).

SRS can take affect over about 40 THz (a very wide range) below the higher frequency (shorter wavelength) involved. That is, it can extend over a range of wavelengths of about 300 nm longer than the shortest wavelength involved. The

effect is maximized when the two frequencies are 13.2 THz apart. SRS increases exponentially with increased power. At very high power it is possible for all of the signal power to be transferred to the Stokes Wave. One study concluded that in a 10-channel WDM system with 1 nm channel spacing power levels need to be kept below 3 mw (per channel) if SRS is to be avoided.

1.2.2 Cross phase modulation

When there are multiple signals at different wavelengths in the same fiber Kerr effect caused by one signal can result in phase modulation of the other signal(s). This is called “Cross-phase Modulation” (XPM) because it acts between multiple signals rather than within a single signal. When N signals propagate through the fiber, the phase of signal at frequency f_i is depends not only its own power but also power of the

signals at other frequency. It is given by [47]
$$\Delta\phi_i(t) = \frac{2\pi n_2 L}{\lambda} \left[I_i(t) + 2 \sum_{j \neq i}^N I_j(t) \right]$$

In contrast to other nonlinear effects XPM effect involves no power transfer between signals. The result can be asymmetric spectral broadening and distortion of the pulse shape. But in presence of dispersion, the phase modulation is converted to intensity modulation leading to crosstalk.

1.2.3 Four wave mixing

One of the biggest problems in WDM systems is called “Four-Wave Mixing” (FWM). FWM occurs when two or more waves propagate in the same direction in the same (single-mode) fiber. The signals mix to produce new signals at wavelengths which are spaced at the same intervals as the mixing signals. This is easier to understand if we use frequency instead of wavelength for the description. A signal at frequency ω_1 mixes with a signal at frequency ω_2 to produce two new signals one at frequency $2\omega_1 - \omega_2$ and the other at $2\omega_2 - \omega_1$. The effect can also happen between three or more signals. If three carrier frequencies ω_1, ω_2 and ω_3 co-propagates in a fiber simultaneously, a fourth wave with frequency $\omega_4 = \omega_1 \pm \omega_2 \pm \omega_3$ is generated. Generally most of these frequencies do not build up due to phase matching requirements and most trouble cross product term is $\omega_4 = \omega_1 + \omega_2 - \omega_3$.

There are a number of significant points:

- The effect becomes greater as the channel spacing is reduced. The closer the channels are together the greater the FWM effect.
- FWM is non-linear with signal power. As signal power increases the effect increases exponentially.
- The effect is strongly influenced by chromatic dispersion. FWM is caused when signals stay in phase with one another over a significant distance. The lasers produce light with a large "coherence length" and so a number of signals will stay in phase over a long distance if there is no chromatic dispersion. Here chromatic dispersion is our friend. The greater the dispersion, the smaller the effect of FWM - because chromatic dispersion ensures that different signals do not stay in phase with one another for very long.
- If the WDM channels are evenly spaced then the new spurious signals will appear in signal channels and cause noise. One method of reducing the effect of FWM is to space the channels unevenly. This mitigates the problem of added noise (crosstalk) in unrelated channels. However, it doesn't solve the problem of the power that is removed from the signal channels in the process.

1.3 THESIS OBJECTIVES AND MOTIVATION

The specific objectives of the present research work for SCM-WDM transmission system are as follows:

- (a) To analyze the effect of crosstalk due to fiber nonlinearity such as XPM, SRS and FWM for different modulation frequency, link length and channel spacing.
- (b) To analyze the BER performance due to combined influence of XPM, SRS and FWM in each wavelength channel.
- (c) To evaluate the BER and power penalty considering all the above mentioned crosstalk.

It is expected that this study will yield an effective analytical strategy to evaluate the performance of a SCM-WDM transmission system and clarify the transmission limitations in presence of fiber nonlinear effects.

1.4 ORGANIZATION OF THESIS

This thesis consists of five chapters. *Chapter-1* deals with introduction to SCM-WDM transmission system, system architecture of an SCM-WDM fiber and nonlinear effects in SCM-WDM Objective of the research and discussion on expected results are also included in this chapter.

Chapter-2 provides a review of existing literatures on SCM system, nonlinear effects of SRS and XPM in SCM-WDM system and FWM effect on WDM system. The need for further research in SCM-WDM system is indicated in this chapter.

Chapter-3 includes the detailed theoretical analysis of the system. The analytical expressions for SRS, XPM and FWM and also the expressions of CNR and BER are presented and explained in this chapter.

Chapter-4 presents simulation results of the analytical expressions. The results are discussed and design considerations are highlighted. In this chapter results are shown consequently for SRS, XPM, FWM effect individually and then also their combined effect.

Chapter-5 concludes this thesis. Suggestions for future work based on the findings of the thesis are also included.

CHAPTER-2

LITERATURE REVIEW

2.1 SUBCARRIER MULTIPLEXED SYSTEM

Subcarrier multiplexing (SCM) is an important new approach to the design of lightwave systems for broad-band distribution. There are several literatures available in this regard.

In [1] the author investigated technologies and design considerations of subcarrier multiplexed (SCM) lightwave systems for subscriber loop applications. State-of-the-art SCM lightwave systems were discussed, together with degradation phenomena which limit the performance of some of these systems.

SCM transmission systems can provide high-capacity and low-cost delivery of both current and future advanced TV signals. Compatibility of SCM technology with existing baseband digital transmission equipment would eliminate the need for a separate analog distribution network and thereby permit a more graceful evolution to a broad-band integrated digital services network (B-ISDN). In [2] the authors considered one version of a hybrid system whereby SCM video and baseband digital signals are simultaneously transmitted by a single laser diode, and the technical issues related to such an implementation. They reported an experiment in which the three color components of a high-definition TV (HDTV) signal, via frequency modulated (FM) microwave subcarriers, were transmitted simultaneously with a baseband 622.08 Mbit/s SONET STS-12 rate data signal by a DFB laser diode over 2 km of single-mode fiber.

The application of broad-band SCM system to both passive and optically amplified distribution networks was discussed in [3]. Performance limiting parameters was mentioned and their impact on carrier to noise ratio (CNR) was also illustrated.

In [4] SCM was used to demonstrate an optical communication system suitable for the distribution of digital video channels. The design, performance, and optical link requirements were discussed for a 2-Gbit/s SCM system with 20 microwave subcarriers modulated at 100 Mbits/s using a frequency shift keyed (FSK) format.

In [5] Incoherent optical subcarrier multiplexing systems were discussed. It was mentioned that in such a system the laser phase noise may cause signal spectrum broadening, and hence, deteriorates the system performance seriously. The authors analyzed the influence of phase noise in terms of carrier to noise ratio, intermodulation distortion, and adjacent channel crosstalk. The optimal modulation index and carrier to noise ratio was also presented.

A method was developed in [6] for calculating carrier-to-intermodulation product ratios for conventional modulators and for linearized modulators in which the third-order products are cancelled, and fifth-order products are dominant. Simple expressions were derived for the rms optical modulation index which optimizes system performance. The improvement in receiver sensitivity which can be achieved with linearized modulators was determined. For AM-VSB systems operating with carrier-to-noise ratios of 50 dB, linearized modulators were predicted to yield an improvement in receiver sensitivity of 8 dB. It was shown that for other SCM system operating with CNR's of 25 dB or less, no performance improvement can be expected.

In [7] the authors described the first wide-band coherent detection optical communications system using two microwave subcarriers to transmit 8 Gb/s with a RF bandwidth efficiency of 1 b/s/Hz. It was demonstrated that two subcarriers each carrying 4 Gb/s QPSK, compactly spaced at just twice the data rate, can achieve a receiver sensitivity of -26.5 dBm with as little as 0.5-dB crosstalk between Subcarriers. They described how the various components impact the overall performance of QPSK/SCM systems including a CNR model for multichannel systems.

Sensitivity improvement of a QPSK SCM system using optical pre amplifier was presented in [8]. About 10 dB sensitivity improvement was reported for direct detection SCM.

Fundamental limitations for EDFA-based subcarrier-multiplexed AM-VSB CATV distribution systems were reported in [9]. The impairments considered were shot noise, amplifier spontaneous emission noise, and laser, clipping-induced, nonlinear distortion. Treating the amplifier input signal power and pump power as resources, authors obtained limits on the number of receivers to which we can deliver at a carrier-to-noise ratio (CNR) of 55 dB (or 48 dB). Moreover, they presented a simple approach that can be used to recalculate the results presented there for different system and amplifier fiber parameters.

In [10] the concept of the subcarrier multiplexed broadband service network (SCM-BSN) was developed in response to the need to provide low-cost integrated broadband services in the local loop. This paper introduced the SCM-BSN concept, described a prototype system that had been built at GTE Laboratories, and described some possible evolutionary scenarios to integrated digital services. While the SCM-BSN prototype system had been designed to provide voice, data, and switched video services using FM-video modulation, the BSN design had been structured to provide for a graceful evolution to other broad-band services including HDTV, digital video, and integrated broad-band services based on ATM transmission.

An analysis of the design factors involved in optimizing laser transmitters for SCM video distribution network was presented in [11]. That includes optimization of the erbium-doped amplifier, linearized external modulation, and laser over modulation to increase the optical loss budget. A full nonlinear distortion spectral analysis was employed to determine the dependence of the optimum optical modulation index on the allowable post amplifier loss. A general optimization procedure was developed for the fiber amplifier and modulator to maximize the post amplifier loss for a specified CNR objective. Results were presented showing a comparison between the distribution capacity of direct and externally modulated SCM-EDFA systems for VSB-AM and FM-SCM transmission systems.

A simple model describing the change in mode partition noise as a function of modulating frequency, modulation depth, and dispersion in a microwave SCM, fiber optic transmission system was presented with experimental verification in [12]. The effects of temperature on laser intensity and mode-partition noise were also explored. Longitudinal mode distribution associated with low and high noise levels were identified.

The second-order intermodulation distortion product, namely composite second-order (CSO) distortion, of an AM-SCM video transmission system can be caused by the optical isolators, cascaded fiber amplifiers, or the fiber transmission cable employed. Moreover, the absolute distortion value depends on the polarization angle of light input to the optical isolators, cascaded fiber amplifiers, and fiber transmission line. The degraded distortion values were measured and their mechanisms were clarified in [13].

In [14] it was found that the presence of the asymmetric nonlinear gain causes the longitudinal modes of a Fabry-Perot laser as well as a nearly single-mode laser to couple such that the low-frequency relative intensity noise is greatly enhanced. For the first time the authors included that asymmetric mode coupling to adequately model the translation of the enhanced low-frequency noise to the signal band of a subcarrier multiplexed transmission system in the presence of both modulation and fiber dispersion. That effect, which is crucial in determining the system's signal-to-noise ratio, was also verified experimentally. Theoretical and experimental investigations of system impairment caused by noise translation and fiber dispersion were also performed. Excellent agreement between the theoretical predictions and the experimental results was obtained.

In [15] authors analyzed the spectrum efficiency and power penalty of multilevel SCM transmission. They found that using pulse shaping can make multilevel signaling attractive. Depending on the ACI that can be tolerated, results showed that multilevel amplitude-shift keying (ASK) of 5-7 b/symbol can give the optimum spectrum efficiency using the raised-cosine pulse. The price paid is a slightly power penalty of 0.4 dB to reduce intersymbol interference (ISI) to zero.

A hybrid scheme was proposed in [16] for the purpose of suppressing the effects of external modulation and/or laser nonlinearities in subcarrier multiplexing (SCM) fiber optic communications systems. Several possible architectures were introduced for the hybrid CDMA/FDMA subcarrier fiber optic local area network (LAN). The networks utilized CDMA and SCM, an asynchronous multiple access scheme. Direct sequence spread spectrum multiple access (DS/SSMA), was employed. It was shown that by using the code sequence sets for which the shift-and-add property holds, intermodulation products and harmonics had a similar interference like effect as non matching sequences do. Owing to the fact that shift-and-add property holds for conventional spreading sequences, suppression of nonlinear distortions was examined. An average error probability performance evaluation of the selected configuration was presented for a transceiver pair. In analysis of the system, authors assumed the interference term arising from other users is Gaussian distributed. The results were compared to that obtained by exact evaluation of interference distribution using Gauss quadrature rule integration (GQR) method. They compared the performance of this scheme for two different code sequence lengths. They also present some preliminary experimental results on the proposed LAN implementation and its measured transmission performance. The results showed promise.

In [17] a new approach was suggested to reduce the optical beat interference (OBI) in subcarrier multiplexed (SCM) wavelength-division multiple access (WDMA) networks. The idea was to deliberately introduce independent random polarization fluctuations in the electric fields transmitted on each optical channel. A two-user system was simulated. Simulation results showed the drastic reduction in OBI power spectral density using appropriate PN signals.

An exact method based on noise theory applied to a fully loaded system in order to evaluate the joint distortion resulting from both laser clipping and the nonlinearity introduced by the carrier heating effects for SCM system is presented in [18]. All orders of distortion were treated and compared with the corresponding cases when the carrier heating effects were suppressed. The resulting carrier-to-nonlinear distortion ratios per channel were presented in graphical form as a function of p and I_b , the laser bias current. The results also confirmed an earlier finding that in the vicinity of

$p = 0.19$, second order distortion limits the performance per channel rather than laser clipping. However, when second order distortion was suppressed, laser clipping again limits the performance per channel. Based on the composite second order (CSO) and composite triple beat (CTB) distortions, it was shown that the optimal total rms modulation index is about $p = 0.25$ for subcarrier multiplexed CATV applications.

In [19] authors considered both the case of using a training sequence to identify the subcarriers to be discarded, and diversity coding in which the information may be recovered in the presence of the loss of a fixed number of subcarriers. Simulation results indicated that diversity coding, which is less complex than the use of training sequences, provides very good performance over a wide range of channel conditions.

A 10-Gb/s SCM long-haul optical system was reported in [20]. 4 2.5 Gb/s data streams were combined into one wavelength, which occupies a 20-GHz optical bandwidth. Optical single sideband was used to increase bandwidth efficiency and reduce dispersion penalty. The receiver sensitivity was calculated using a simplified receiver model with an optical preamplifier. The measured results agree well with the analytical prediction.

The performance of high-speed digital fiber-optic transmission using subcarrier multiplexing (SCM) was investigated both analytically and numerically in [21]. In order to optimize the system performance, tradeoffs must be made between data rate per subcarrier, levels of modulation, channel spacing between subcarriers, optical power, and modulation indexes. A 10-Gb/s SCM test bed was set up in which 4 2.5 Gb/s data streams were combined into one wavelength that occupies a 20-GHz optical bandwidth. OSSB modulation was used in the experiment. The measured results agree well with the analytical prediction.

2.2 FIBER NONLINEAR EFFECTS IN SCM/WDM

Combination of SCM with WDM is a new technology to serve broad band services to a large number of subscribers. The main problem of the system is nonlinear crosstalk which degrades the system performances. So, research is going on analysis of nonlinear crosstalk, its impact on system performance, countermeasure of crosstalk and optimization of system parameters.

Crosstalk induced by Stimulated Raman Scattering (SRS) and Cross Phase modulation (XPM) was analyzed individually for SCM/WDM in [22] and [23] respectively. The authors presented analytical expressions for SRS and XPM. Performance degradation imposed by SRS and XPM were reported for video distribution system.

In [24] crosstalk in a two-wavelength 1550-nm standard fiber system at subcarrier frequencies 50–800 MHz was investigated. The dependence of the crosstalk on subcarrier frequency, wavelength spacing, and optical power was measured and analyzed. The observed crosstalk was attributed to three primary mechanisms: stimulated Raman scattering, cross-phase modulation, and the optical Kerr effect combined with polarization-dependent loss. It was found that at wavelength spacing greater than 9 nm, stimulated Raman scattering dominates. At wavelength spacing less than 5 nm, the primary contributor can be the optical Kerr effect with polarization dependent loss, except at higher modulation frequencies where cross-phase modulation also is significant.

In [25] the authors investigated, theoretically and experimentally, crosstalk between wavelengths in subcarrier-multiplexed (SCM) wavelength-division multiplexed (WDM) optical communication systems. They considered crosstalk from interactions between subcarriers on one wavelength and the optical carrier of another wavelength and crosstalk due to stimulated Raman scattering (SRS) and cross-phase modulation (XPM) combined with group velocity dispersion (GVD). They investigated the phase relationship between SRS-induced and XPM-induced crosstalks. Crosstalks induced by SRS and XPM add in the electrical domain and can interfere constructively or destructively. Experimental results showed that the combined crosstalk level can be as

high as 40 dBc after 25 km of SMF with two wavelengths and 18 dBm per wavelength of transmitted power. They also proposed two crosstalk countermeasures. The first countermeasure was using parallel fiber transmission. It was theoretically shown that both SRS-induced and XPM-induced crosstalks can be canceled to the first order. An experimental demonstration of concept which has achieved 15 dB of crosstalk cancellation over 200 MHz was presented.

The second countermeasure was using optical carrier suppression. They showed, theoretically and experimentally, that by suppressing the optical carrier, one can significantly reduce crosstalk while maintaining the same link budget and carrier-to-noise ratio (CNR) at the receiver. 20 dB of crosstalk reduction over 2 GHz was demonstrated experimentally.

In [26] the authors presented an analytic approach to optimizing the information capacity of a subcarrier- Multiplexed wavelength-division- multiplexed optical communication link. Receiver and relative-intensity noise, clipping distortion, and crosstalk between wavelength channels due to optical nonlinearities in the fiber were the signal impairments considered.

The transmission limitation of multiple narrow single-sideband subcarrier-multiplexed (SSB/SCM) signals, in [27] it was first presented a closed-form analysis to predict Mach-Zehnder intensity modulator-induced composite triple beat (CTB), and linear-fiber-dispersion-induced composite second-order (CSO) and CTB distortions. To combine SSB/SCM with dense-wavelength-division-multiplexing (DWDM) systems, analytical and numerical tools were used to analyze cross-phase modulation-induced crosstalk. All the analytical and numerical results were verified by computer simulations. Several multichannel SSB/SCM/DWDM systems with transport capacities of 10 or 20 Gb/s per wavelength, with a wavelength spacing of 25, 50, and 100 GHz, were also studied in that paper to understand the fundamental transmission limitations.

In [28] theoretical investigations for crosstalk between the channels of SCM-WDM optical communication system were reported. The crosstalk was evaluated including the impact of SRS and XPM. Further the XPM induced crosstalk was evaluated by including the influence of was evaluated by including the higher order dispersion. Moreover it was observed that SRS crosstalk was dominating over XPM.

Effect of XPM in SCM/WDM microcellular system was investigated in [29]. Crosstalk variations with different transmission parameters and BER performance were evaluated. It was found that XPM induced crosstalk is directly proportional to link length and modulation frequency and inversely proportional to WDM channel spacing.

2.3 FOUR WAVE MIXING IN WDM SYSTEM

In last few years effect of FWM is reported in some literatures [30-39]. Most of them describes performance degrading effect of FWM and countermeasures of FWM.

In [30] fiber four-wave mixing (FWM) in the zero dispersion wavelength region was described. The phase-matching characteristics were studied in the wavelength region where the first-order chromatic dispersion is zero. The results showed that the phase-matching condition was satisfied and FWM light was efficiently generated at particular combinations of input light wavelengths. It was also shown that the deviation of the zero dispersion wavelength along the fiber length plays an important role in FWM behavior.

Channel crosstalk due to fiber four-wave mixing (FWM) in multichannel systems operated around the zero dispersion wavelength was experimentally studied in [31]. After determining the wavelength at which FWM light was most efficiently generated, the FWM efficiency was measured for possible frequency combinations which generate FWM light at that wavelength. Using those data, FWM crosstalk in multiwavelength systems was evaluated. The results showed that actual crosstalk was less than the value estimated by the theoretical model assuming the uniformly

distributed chromatic dispersion for 80-km-long fibers. It is concluded that the theoretical model can be applied to system design dealing with the worst condition.

The influence of fiber four-wave mixing on multichannel transmissions was investigated in [32]. The authors presented strict and approximate theoretical treatments for evaluating power penalty with intensity-modulated/direct-detection (IM/DD) and FSW direct detection.

A comparison of calculations showed that both methods yield the same result in the small penalty region. Using those treatments, power penalty and allowable fiber input power were derived for various system conditions. It was shown that the power penalty is not uniquely determined by the crosstalk level for CW lights, depending on the demodulation scheme and channel spacing, especially in the zero-dispersion wavelength region.

In [33] a theoretical model was presented for analyzing the propagation of densely spaced WDM optical signals through a cascade of erbium-doped fiber amplifiers and single-mode optical fibers with non uniform chromatic dispersion. By combining a numerical solution for the EDFA and an analytical expression for FWM components generated through the cascade, the model allowed a realistic system analysis which includes gain peaking effect, amplified spontaneous emission accumulation and the effect of dispersion management on the four-wave mixing efficiency. The FWM power distribution at the end of the multi amplifier transmission link was computed taking into account the phase relation between FWM light amplitudes generated within different sections of the link. The transmission of many WDM channels, evenly spaced around 1547.5 nm, was analyzed for various dispersion management techniques and propagation distances. Numerical results pointed out the importance of such a model for a realistic design of WDM optical communication systems and networks. It was found that a proper choice of chromatic dispersion, amplifier characteristics, span length, input signal powers and wavelengths, combined with the use of gain equalizing filters, allows maximizing the transmission distance ensuring acceptable signal-to-noise ratio (SNR) and limited SNR variation among channels.

In [34] for WDM systems over nonzero dispersion fiber, the authors evaluated the statistics of the eye-closure due to FWM in the presence of arbitrary data values and optical phases in all WDM channels. By Monte Carlo (MC) experiments, they determined the distribution function and the standard deviation of the eye-closure for several channel counts. Convolution of the distribution after a single span yields the eye-closure distribution after multiple amplified spans. The results were used to assess the Q-factor penalty in a WDM system. The limits for optical power, chromatic dispersion and channel spacing then found. It was shown that the power of the FWM products can be used to estimate the system penalty due to FWM.

When comparing standard single-mode fiber with nonzero dispersion-shifted fiber (NZDSF), they found that standard fiber allows for triple narrower channel spacing than NZDSF, given the same set of system parameters.

A new phase-matching factor was derived in [35] for FWM that includes the effects of self-phase and cross-phase modulation in optical fibers. Theoretical results showed that the wavelength of peak FWM efficiency shifts away from the fiber zero-dispersion wavelength and indicated that the conventional phase-matching factor may induce significant errors in FWM calculations. Experiments were presented to verify the new phase-matching factor and the related theoretical results. The measured results agreed well with those predicted by the new phase-matching factor.

New analytical tools to calculate the variance due to cross-phase modulation (XPM) and four-wave mixing (FWM) induced intensity distortion were derived based on the Volterra series transfer function method in [36]. The analysis for both the XPM and FWM effects was based on the same system configuration with a continuous-wave (CW) probe channel plus modulated pump channels, which makes possible a fair comparison between the two nonlinear effects. Effective ways to reduce the XPM- and FWM-induced intensity distortion were given. The new results on the variance of the nonlinearity-induced intensity fluctuation also was studied both synchronous wavelength-division multiplexing (WDM) systems with fixed channel delays and asynchronous WDM systems with random channel delays. The new analytical results provided accurate and efficient ways for system parameter optimization to reduce these two nonlinear effects.

In [37] transmission performance of ultra-dense 2.5- and 10-Gb/s non return-to-zero intensity-modulated direct-detection wavelength-division-multiplexing systems in various single-mode fibers was investigated. Fundamental limiting factors and their remedies by using optimum dispersion compensation for periodically amplified systems in band were presented. The three fundamental limiting factors in U-DWDM systems considered were - various random noise terms, fiber chromatic dispersion-induced intersymbol interference (ISI), and optical-nonlinearity-induced distortion and interference.

A noise theory for FWM tone generated by nonlinear interaction of channels of a wavelength-division- multiplexed system was described in [38]. Analytical expressions for power spectral density and variance of FWM noise were derived without ignoring group-velocity walk-off between channels. The results showed that the variance of FWM noise exhibits sharp minima and maxima as a function of channel separation which is due to the coherent interaction between channels. When the walk-off distance is large or comparable to effective fiber length, FWM penalty can be reduced by introducing a suitable initial delay between interacting channels.

In order to reduce FWM-induced distortion two new techniques, the hybrid amplitude-/frequency-shift keying (ASK/FSK) modulation and the use of pre chirped pulses were investigated in [39]. It was shown that both techniques can greatly improve the Q -factor in a 10 Gb/s WDM system. That happens even for very high input powers (10 dBm), where the degradation of the conventional WDM system is prohibitively high. The proposed methods were also applied and tested in higher bit rates (40 Gb/s). It is deduced that although the hybrid ASK/FSK modulation technique marginally improves the system performance, the optical pre chirp technique can still be used to greatly increase the maximum allowable input power of the system.

2.4 SUMMARY

From the literatures describing SCM system it is clear that only SCM is not enough to use the enormous bandwidth of fiber optic cable. So combination of SCM with WDM is a more advantageous technique. But introducing WDM with SCM causes crosstalk leading to performance degradation.

In all experiments performed, only two wavelengths have been used presumably due to difficulties that arise out of implementing a large scale system. But it is necessary to analyze multi channel system to find out mostly affected channel. Because XPM induced crosstalk is mostly affect central wavelength channel while highest wavelength channel is mostly affected by SRS. So, it is necessary to analyze both the channels while considering both XPM and SRS.

Again, the literatures so far described, considered only SRS and/or XPM as fiber nonlinear effect as they considered dispersive fiber. Several methods have been discussed to compensate these effects such as uses of parallel fiber, carrier power suppression, uses of multi segment system etc. The literatures that consider CNR and BER performance analysis taking XPM and SRS in account are limited. SCM-WDM system using DSF is also limitedly described in literatures.

Though several literatures mentioned effect of FWM in WDM system, its effect in SCM-WDM system is yet to be reported. So, further study is required for analysis of performance of an SCM-WDM system, in presence of combined influence of all the fiber nonlinear effects namely XPM, SRS and FWM.

CHAPTER-3

THEORETICAL ANALYSIS

3.1 SCM-WDM SYSTEM ARCHITECTURE

The block schematic of a basic subcarrier multiplexed system is shown in Fig.3.1.

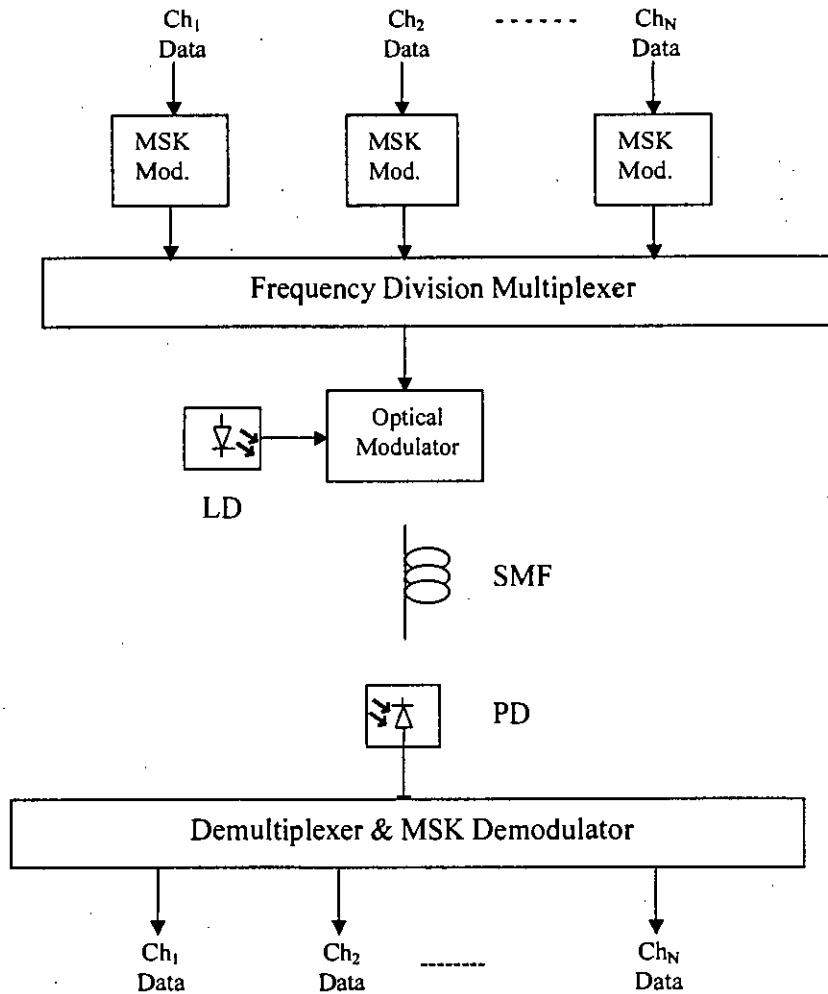


Fig.3.1: Diagram of subcarrier multiplexed lightwave system

The modulated microwave subcarrier signals are obtained modulating the baseband signal using an analog or digital modulation technique. In this thesis MSK is used for subcarrier modulation. These subcarrier signals f_i are then summed in a frequency division multiplexer prior to the application of composite signal to an injection laser which is dc biased in order to produce desired intensity modulation. The IM optical signal is then transmitted over single mode fiber and directly detected using a wideband photodetector before demultiplexing and demodulation using a conventional receiver.

The basic configuration of an SCM-WDM transmission system is shown in Fig.3.2. In the figure n independent base band signals are mixed by N different microwave frequencies f_i . These are combined to produce SCM composite signals and then optically intensity modulated onto an optical carrier. M wavelengths are then multiplexed together in an optical WDM configuration. At the receiver an optical demultiplexer separates the wavelengths for individual optical detectors. Then RF coherent detection is used at the SCM level to separate the base band signals.

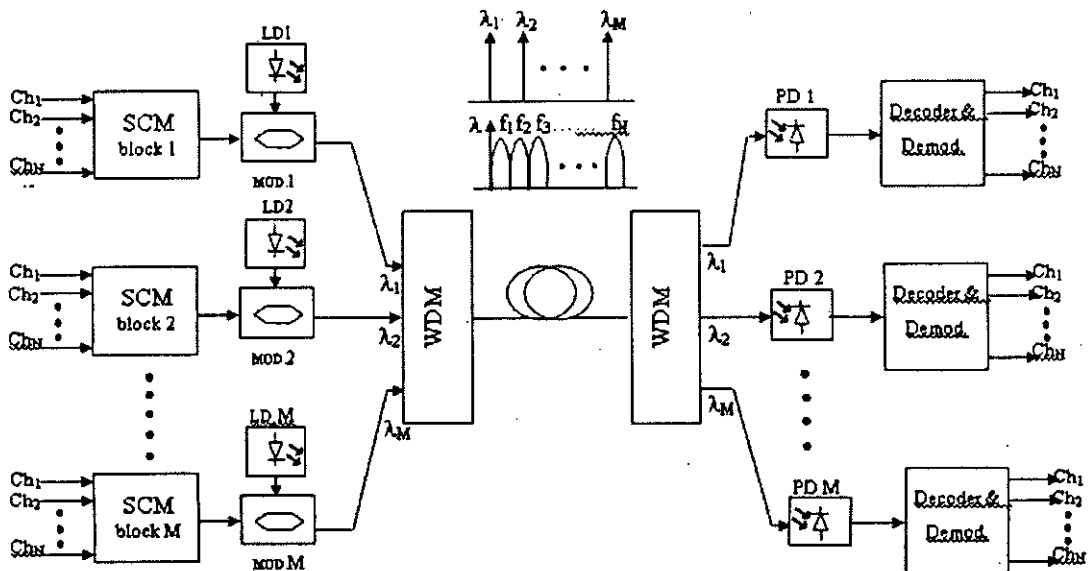


Fig 3.2 SCM-WDM system architecture

Compare to conventional high speed TDM systems, SCM is less sensitive to fiber dispersion because the dispersion penalty is determined by the width of the base band of each individual signal channel. Compared to conventional WDM system, on the other hand, it has better optical spectral efficiency because much narrow channel spacing is allowed.

3.2 SYSTEM DESCRIPTION AND OPERATION

Referring to Fig.3.2, if Minimum Shift Keying (MSK) is used for subcarrier modulation then, the SCM signal to the optical modulator can be expressed as

$$S_{SCM}(t) = \sum_{i=1}^N S_{MSK_i}(t) \quad (3.1)$$

where $S_{MSK}(t)$ can be expressed as

$$S_{MSK}(t) = \sqrt{\frac{2E_b}{T_b}} \cos[2\pi f_c t + \theta(t)]$$

The nominal carrier frequency f_c is chosen as the arithmetic mean of two frequency f_1 and f_2 , as shown by

$$f_c = \frac{1}{2}(f_1 + f_2)$$

The phase $\theta(t)$ increases or decreases linearly with time during each bit period, as shown by

$$\theta(t) = \theta(0) \pm \frac{\pi h}{T_b} t$$

Where + sign corresponds to symbol 1 and – sign for 0. The deviation ratio h can be expressed as

$$h = T_b(f_1 - f_2)$$

For MSK, value of h is $\frac{1}{2}$.

The composite SCM signal expressed in equation (3.1), which is a summation of all the individually MSK modulated signals, is added to the bias current of a semiconductor laser in order to directly intensity modulated it.

This intensity modulated signal comprises a single WDM wavelength channel. The transmitted signal at λ_k wavelength is given as in [47],

$$S_k(t) = \sqrt{P_b \left[1 + \sum_{i=1}^N m_i S_{SCM_i}(t) \right]} \quad (3.2)$$

where, P_b is the output power at bias level at for k_{th} wavelength channel's semiconductor laser. It is assumed that P_b is constant for all wavelength channels and m_i , denoting the optical modulation index, is also constant.

M such signals are then placed on different wavelengths on a single mode fiber. The optical carriers are multiplexed by wavelength division multiplexer (WDM). A composite optical signal of M nominal wavelengths $\lambda_1, \lambda_2, \lambda_3 \dots \lambda_M$ is produced by WDM and this signal is transmitted over a single fiber. The expression of the wavelength division multiplexed system is given by

$$S_{WDM}(t) = \sum_{k=1}^M S_k(t) \quad (3.3)$$

At the receiving end, a demultiplexer separates all optical carriers for individual optical detectors. The total signal power received at the photo detector can then be written as

$$P_k = P_b \left[1 + \sum_{i=1}^N m_i S_{MSK_i} \right] \quad (3.4)$$

Each optical signal is converted to the corresponding electrical signal through Direct Detection (DD) by using a photodiode detector. Taking all the noise factors and crosstalk due to fiber nonlinearity in consideration the total photo current obtained at the output of the photo detector is given by

$$\begin{aligned} i(t) &= R_d S_k^2 + i_{shot} + i_{thermal} + i_{intensity} + i_{XT} \\ &= R_d P_k + i_{shot} + i_{thermal} + i_{intensity} + i_{XT} \end{aligned} \quad (3.5)$$

i_{shot} is the shot noise current, which is small leakage current that is present when there is no optical power incident on the photo diode, $i_{thermal}$ is the thermal noise current caused by the spontaneous fluctuation due to thermal fluctuation in the photo detector, $i_{intensity}$ is relative intensity noise current caused by the intensity fluctuation at the laser diode output and i_{XT} is the current due to fiber nonlinear crosstalk. R_d is the photodiode responsivity of the k_{th} photo detector. This parameter gives the

information of photon electron conversion efficiency of the photo detector and is given by

$$R_d = \frac{\eta e}{hf}$$

Where η corresponds to quantum efficiency, e is the charge of electron and h is plank's constant.

This detected signal is then pass through a band pass filter to filter out the noises. At this point SCM signal is found in electrical domain. This signal is then demultiplexed using a SCM demultiplexer. Here the SCM signal is resolved into N subcarriers RF signals. These signals are then demodulated coherently and filtered to get original signal.

3.3 SRS INDUCED CROSSTALK

Stimulated Raman scattering (SRS) is a nonlinear phenomena found in the WDM system. As shown in Fig. 3.3 the shorter wavelength channels are robbed of power and that power is feeds to the longer wavelength channel [22].

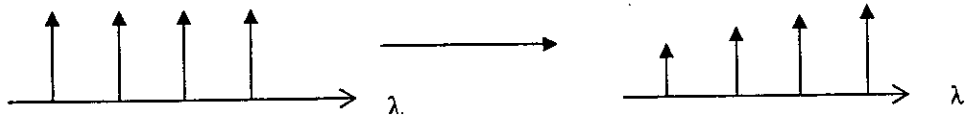


Fig 3.3: SRS induced crosstalk

A formal approach for determining SRS crosstalk level is to solve the coupled equation for optical intensity I at wavelength λ_j and λ_k [24]-

$$\frac{\partial I_j}{\partial z} + \frac{1}{v_j} \cdot \frac{\partial I_j}{\partial z} = (g_{jk} I_k - \alpha) I_j \quad (3.6)$$

$$\frac{\partial I_k}{\partial z} + \frac{1}{v_k} \cdot \frac{\partial I_k}{\partial z} = (-g_{jk} I_j - \alpha) I_k \quad (3.7)$$

Where z is the distance along the fibre, g is the Raman gain co-efficient and v is the group velocity of each wavelength channel.

Consider $\lambda_j > \lambda_k$ and both the optical waves co-propagate in the fibre with same polarisation.

Using the effective mode area approximation $I = \frac{P}{A_{eff}}$, where P is the power-

$$P_j = P_j(0, u_j) e^{-\alpha} \exp\left[\frac{g_{jk}}{A_{eff}} \int_0^z P_k(0, u_j + d_{jk} z') e^{-\alpha'} dz'\right]$$

$$\approx P_j(0, u_j) e^{-\alpha} \cdot \left[1 + \frac{g_{jk}}{A_{eff}} \int_0^z P_k(0, u_j + d_{jk} z') e^{-\alpha'} dz'\right]$$

Where $u_j = t - \frac{z}{v_j}$ and the exponential is assumed to first order and d_{jk} is the walk-off

parameter and related to dispersion coefficient D by

$$d_{jk} = \frac{1}{v_j} - \frac{1}{v_k} \approx D(\lambda_j - \lambda_k).$$

Consider modulated wave channel k has power $P_k = P_0(1 + \cos \omega t)$ and both channels have same average optical power -

$$P_j = P_0 e^{-\alpha} \left\{ 1 + \frac{g_{jk} P_0 L_{eff}}{A_{eff}} + \frac{g_{jk} P_0 m}{A_{eff}} \times \frac{\sqrt{1 + e^{-\alpha} - 2e^{-\alpha} \cos(\omega d_{jk} z)}}{\sqrt{\alpha^2 + (d_{jk} \omega)^2}} \times \cos(\omega u_1 + \theta_{SRS}) \right\} \quad (3.8)$$

$$\text{Here, } \theta_{SRS} = \tan^{-1}\left(\frac{-d_{jk} \omega}{-\alpha}\right) + \tan^{-1}\left(\frac{e^{-\alpha} \sin(\omega d_{jk} z)}{e^{-\alpha} \cos(\omega d_{jk} z) - 1}\right) \quad (3.9)$$

L_{eff} is the effective length of fibre and is given by

$$L_{eff} = \frac{1}{\alpha} (1 - e^{-\alpha}) \quad (3.10)$$

From equation (3.8) the first term corresponds to the carrier power after loss. The second term corresponds to the interaction between the optical carriers, this result as optical dc power loss or gain. The third term is the crosstalk as the result of power depletion through SRS from low wavelength optical channel to high wavelength optical channel.

Hence, the crosstalk in j^{th} channel due to k^{th} channel is:

$$\begin{aligned}
 XT_{(SRS)jk} &= \left\{ \frac{\left(\frac{d_{jk} P_0}{A_{\text{eff}}} \right)^2 \frac{1 + e^{-2\alpha} - 2e^{-\alpha} \cos(\omega d_{jk} z)}{(\alpha^2 + \omega^2 d_{jk}^2) \left(1 + \frac{g_{jk} P_0 L_{\text{eff}}}{A_{\text{eff}}} \right)^2}}{\left(\frac{d_{jk} P_0}{A_{\text{eff}}} \right)^2 \frac{1 + e^{-2\alpha} - 2e^{-\alpha} \cos(\omega d_{jk} z)}{(\alpha^2 + \omega^2 d_{jk}^2)}} \right\} \\
 &\approx \left\{ \frac{\left(\frac{d_{jk} P_0}{A_{\text{eff}}} \right)^2 \frac{1 + e^{-2\alpha} - 2e^{-\alpha} \cos(\omega d_{jk} z)}{(\alpha^2 + \omega^2 d_{jk}^2)}}{\left(\frac{d_{jk} P_0}{A_{\text{eff}}} \right)^2 \frac{1 + e^{-2\alpha} - 2e^{-\alpha} \cos(\omega d_{jk} z)}{(\alpha^2 + \omega^2 d_{jk}^2)}} \right\} \quad (3.11)
 \end{aligned}$$

Now, for a WDM system with M number of channels such that $\lambda_1 < \lambda_2 < \dots < \lambda_M$, crosstalk in j^{th} channel due to SRS can be expressed as

$$XT(SRS)_j = \sum_{k=1}^{j-1} XT_{(SRS)jk} - \sum_{k=j+1}^M XT_{(SRS)jk} \quad (3.12)$$

Here first term related to power gain of channel j from shorter wavelength channels leading to crosstalk whereas second term related to power depletion of channel j to higher wavelength channels.

Hence for equal power in each channel and equal channel spacing, from equation (3.12) it is clear that for an odd number of WDM channels XT_{SRS} in central wavelength channel is zero and shorter than that wavelength channels deplete power whereas higher wavelength channels than that gain power to create crosstalk due to SRS. For M being an even number the first half shorter wavelength channels deplete power and other half suffers crosstalk.

3.4 XPM INDUCED CROSSTALK

XPM originates from the Kerr effect in optical fibres, where the intensity modulation of one optical carrier can modulate the phase of other co-propagating optical signals in the same fibre. In presence of dispersion, the phase modulation is converted to intensity modulation leading to crosstalk.

The non-linear phase induced in λ_j channel, neglecting any power distortion in the field of λ_k channel is

$$\Phi_{NLj}(z, u_j) = -2\gamma_j \int_0^z P_k(z', u_j + d_{jk} z') dz' \quad (3.13)$$

Where, γ_j is the non-linear coefficient related to non-linear refractive index n_2 by

$$\gamma_j = \frac{2\pi n_2}{\lambda_j A_{eff}} \quad (3.14)$$

Let, $A(z, u)$ denote the slowly varying field envelop of each wave such that,

$$A(z, u) = \sqrt{\frac{P(z, u)e^{-\alpha z}}{A_{eff}}} \cdot \exp(i\Phi(z, u))$$

$$P(z, u) = P_0(0, u) + \Delta P(z, u)$$

$$\Phi(z, u) = \Phi_0(z, u) + \Delta\Phi(z, u)$$

Where intensity of the field is represented as $|A|^2$, P_0 and Φ_0 are the power and phase unperturbed by chromatic dispersion. The above expressions are substituted into the linear wave equation [40]-

$$\frac{\partial A}{\partial z} + \frac{1}{v} \frac{\partial A}{\partial t} - \frac{i}{2} \beta_2 \frac{\partial^2 A}{\partial t^2} + \frac{\alpha}{2} A = 0 \quad (3.15)$$

Where, $\beta_2 = \frac{-\lambda^2 D}{2\pi c}$. The first iteration of the equation yields a change in power given by

$$\Delta P(z, u) = -\beta_2 \int_0^z dz' \left\{ P_0(0, u) \frac{\partial^2 \Phi_0(z, u)}{\partial u^2} + \frac{\partial P_0(0, u)}{\partial u} \frac{\partial \Phi_0(z', u)}{\partial u} \right\} \quad (3.16)$$

Now, substituting $\Phi_0(z, u_j) = \Phi_0 + \Phi_{NLj}(z, u_j)$ in the above equation the output equation is given by

$$\begin{aligned} P_j(z, u_j) &= P_0 e^{-\alpha z} \left[1 - \beta_2 \frac{\partial^2}{\partial u_j^2} \int_0^z \Phi_{NLj}(z'', u_j) dz'' \right] \\ &= P_0 e^{-\alpha z} \left\{ 1 - 2\beta_2 \omega^2 \gamma_m P_0 \times \frac{\sqrt{(e^{-\alpha z} \cos(d_{jk} \omega z) - 1 + \alpha z)^2 + (e^{-\alpha z} \sin(d_{jk} \omega z) - d_{jk} \omega z)^2}}{\alpha^2 + (d_{jk} \omega)^2} \cos(\omega u_j + \theta_{xpm}) \right\} \end{aligned} \quad (3.17)$$

$$\text{Here } \theta_{xpm} = \tan^{-1} \left(\frac{2d_{jk} \omega \alpha}{\alpha^2 - (d_{jk} \omega)^2} \right) + \tan^{-1} \left(\frac{e^{-\alpha z} \sin(d_{jk} \omega z) - d_{jk} \omega z}{e^{-\alpha z} \cos(d_{jk} \omega z) - 1 + \alpha z} \right) \quad (3.18)$$

Hence from the equation (3.17) crosstalk in λ_j channel for λ_k channel can be derived as

$$XT_{(xpm),jk} = (2\beta_2 \omega^2 \gamma_j P_0)^2 \left(\frac{1 + e^{-2\alpha z} - 2e^{-\alpha z} (1 - \alpha z) \cos(d_{jk} \omega z) - 2z[\alpha + d_{jk} \omega e^{-\alpha z} \sin(d_{jk} \omega z)] + [\alpha^2 + (d_{jk} \omega)^2 z^2]}{[\alpha^2 + (d_{jk} \omega)^2]^2} \right) \quad (3.19)$$

For an M channels WDM system crosstalk due to XPM in j^{th} channel from other channels can be expressed by

$$XT_{(XPM)j} = \sum_{k=1, k \neq j}^M XT_{(XPM)jk} \quad (3.20)$$

3.5 CONSTRUCTIVE & DESTRUCTIVE SRS+XPM CROSSTALK CONCEPT

Consider $\lambda_j > \lambda_k$, then λ_k provides the Raman gain. λ_j channel results in modulated gain through SRS interaction between λ_j and λ_k (Fig. 3.4a). Intensity modulation of λ_k creates a phase modulation to λ_j because of optical Kerr effect and then converts to IM with fibre dispersion. Therefore, crosstalk in λ_j from SRS and XPM are in phase with each other and add constructively.

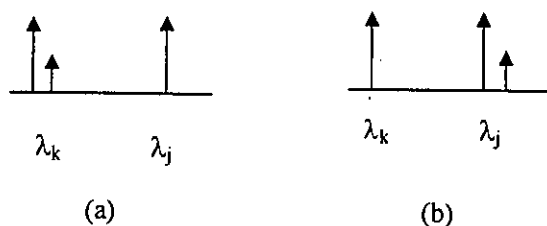


Fig.3.4: Demonstration of constructive and destructive concept of SRS+XPM crosstalk.

On the other hand, if $\lambda_j < \lambda_k$ then λ_j channel losses power to λ_k . λ_j channel results in modulated depletion through SRS interaction between λ_j and λ_k (Fig.3.4b). XPM is induced as before. Hence crosstalk in λ_j from SRS and XPM are out of phase with each other and add destructively.

3.6 FWM INDUCED CROSSTALK

When an intense field is applied to a dielectric medium, the bound electrons respond with anharmonic motion. As a result the induced polarization in the medium is not a simple linear function of the applied field, but becomes higher order products of the field. FWM interaction is an example of such a process which occurs due to third-order nonlinear susceptibility. Although the third order susceptibility in glass is quite weak, FWM in fiber may be very strong due to large field intensities in the core and the long interaction lengths.

Let three signals are co-propagating at frequencies f_i, f_j, f_k through a single mode fiber. Through the nonlinear interaction, a four-wave mixing signal will be generated at frequency $f_{ijk} = f_i + f_j - f_k$. If we assume that input signals are not depleted by the generation of new of mixing products, the magnitude of this new optical signal is given by [32]:

$$P_{ijk}(f) = \frac{1024\pi^6}{n^4 \lambda^2 c^2} \left(\frac{D_e \chi_{1111} L_{eff}}{A_{eff}} \right)^2 P_i(f) P_j(f) P_k(f) e^{-\alpha z} \quad (3.21)$$

Here, $P_i(f)$, $P_j(f)$ and $P_k(f)$ represent power spectral density (PSD) of i-th, j-th and k-th channel respectively, n is the fiber core refractive index, z is the link length, χ_{1111} is the third order nonlinear susceptibility, D_e is the degeneracy factor equals 3 for two tone products ($i = j$, degenerate FWM) and 6 for three tone products ($i \neq j$, degenerate FWM).

The FWM efficiency can be expressed as

$$\eta = \left| \frac{1 - e^{-(\alpha - i\Delta\beta)z}}{L_{eff}(\alpha - i\Delta\beta)} \right|^2 \quad (3.22)$$

Using the value of L_{eff} from equation (3.10), equation (3.22) can be rewritten as

$$\begin{aligned} \eta &= \frac{\alpha^2}{\alpha^2 + \Delta\beta^2} \times \frac{\{1 - e^{-(\alpha - i\Delta\beta)z}\} \{1 - e^{-(\alpha + i\Delta\beta)z}\}}{(1 - e^{-\alpha z})^2} \\ &= \frac{\alpha^2}{\alpha^2 + \Delta\beta^2} \left[1 + \frac{2e^{-\alpha z} [1 - \cos(\Delta\beta z)]}{(1 - e^{-\alpha z})^2} \right] \\ &= \frac{\alpha^2}{\alpha^2 + \Delta\beta^2} \left[1 + \frac{4e^{-\alpha z} \sin^2(z\Delta\beta/2)}{(1 - e^{-\alpha z})^2} \right] \end{aligned} \quad (3.23)$$

Where, $\Delta\beta$ represents the phase mismatch and can be expressed in terms of signal frequency differences:

$$\Delta\beta = \frac{2\pi\lambda^2}{c} \Delta f_{ik} \Delta f_{jk} \left[D + \frac{\lambda^2}{2c} (\Delta f_{ik} + \Delta f_{jk}) \frac{dD}{d\lambda} \right] \quad (3.24)$$

Here, $\Delta f_{ik} = |f_i - f_k|$ and $\Delta f_{jk} = |f_j - f_k|$.

The nonlinear susceptibility χ_{1111} is related to the fiber nonlinear refractive index n_2 by the relation [35]:

$$n_2 = \frac{48\pi^2}{cn^2} \chi_{1111} \quad (3.25)$$

Hence, to evaluate FWM induced crosstalk equation (3.21) can be expressed in terms of n_2 and nonlinear coefficient γ by

$$P_{ijk}(f) = \frac{\eta}{9} D_e^2 \gamma^2 P_i(f) P_j(f) P_k(f) L_{eff}^2 e^{-\alpha} \quad (3.26)$$

3.6.1 FWM Crosstalk in SCM-WDM System

In this thesis, a new analytical technique is proposed to determine the FWM generated power in an SCM-WDM transmission system. Consider the spectrum of fiber input power as shown in Fig.3.3. Here optical single side band modulation (OSSB) has been considered. OSSB signal can be generated by applying the composite modulating signal from an SCM block to both electrodes of the MZI modulator, with a relative $\frac{\pi}{2}$ phase shift between the arms. A dc bias sets the modulator at a quadrature point.

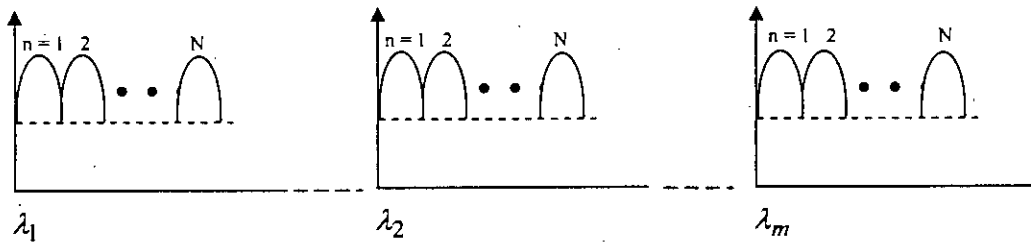


Fig. 3.5: Power Spectrum in fiber input power.

To evaluate the FWM crosstalk among the subcarriers of different WDM channels, equation (3.26) is used. Referring to Fig. 3.5 the PSD of n -th subcarrier channel can be expressed as:

$$P_n(f) = P_b / N + m_n |S_{MSK}(f)_n|^2 \quad (3.27)$$

If MSK is used to modulate subcarrier then following [49], $S_{MSK}(f)$ can be written as:

$$S_{MSK}(f) = \frac{32E_b}{\pi^2} \left[\frac{\cos(2\pi T_b f)}{16T_b^2 f^2 - 1} \right]^2 \quad (3.28)$$

Three subcarriers are chosen from three different λ channels at time to evaluate P_{ijk} and total crosstalk will be summation of all P_{ijk} for all possible combinations. Total possible combinations are ${}^N C_1 \times {}^M C_3 \times N^2$.

To find out the number of combinations form M number of wavelength channels each having N subcarriers, consider first three wavelength channels. At first, 1st subcarrier of λ_1 and 1st subcarrier of λ_2 are kept constant while 1st to N^{th} subcarrier from λ_3 is taken consecutively to form first N combinations. Then while 1st subcarrier of λ_1 is chosen and 2nd to N^{th} subcarrier of λ_2 are taken and again for each subcarrier of λ_2 channel 1st to N^{th} subcarrier from λ_3 is taken. Then for variation of 2nd to N^{th} subcarrier in λ_1 channel, 1st to N^{th} subcarrier from λ_2 is chosen for each subcarrier in λ_1 channel and also 1st to N^{th} subcarrier from λ_3 is varied for each subcarrier of λ_2 channel.

Then 3rd wavelength channel is chosen from λ_4 to λ_M and for each λ value different combinations of subcarriers are find out as before. Then 2nd λ channel is varied from λ_3 to λ_{M-1} and for each channel variation 3rd wavelength channel is chosen from next wavelength channel to λ_M . Then first wavelength channel is taken from λ_2 to λ_M and for each channel variation 2nd λ channel is chosen from next wavelength channel to λ_{M-1} and also for each channel variation 2nd wavelength channel, 3rd λ channel is taken from next wavelength channel to λ_M . For each three λ combinations, subcarriers combinations are chosen as described before.

For example, consider three channel WDM system each having 2 subcarriers. Then, total possible combinations are shown in Table 3.1.

Table 3.1

Possible combinations to evaluate FWM crosstalk for M= 4& N=2

M1	M2	M3	M4
N1	N1	N1	
N1	N1	N2	
N1	N2	N1	
N1	N2	N2	
N2	N1	N1	
N2	N1	N2	
N2	N2	N1	
N2	N2	N2	
N1	N1		N1
N1	N1		N2
N1	N2		N1
N1	N2		N2
N2	N1		N1
N2	N1		N2
N2	N2		N1
N2	N2		N2
N1		N1	N1
N1		N1	N2
N2		N2	N1
N2		N2	N2
N1		N1	N1
N1		N1	N2
N2		N2	N1
N2		N2	N2
	N1	N1	N1
	N1	N1	N2
	N1	N2	N1
	N1	N2	N2
	N2	N1	N1
	N2	N1	N2
	N2	N2	N1
	N2	N2	N1

3.7 CNR & BER CALCULATION

Carrier to noise ratio (CNR) in a RF channel of an SCM/WDM transmission system can be expressed as

$$CNR = \frac{(R_d \mu P_r)^2}{N(\sigma_{th}^2 + \sigma_{shot}^2 + \sigma_{intensity}^2 + \sigma_x^2)} \quad (3.29)$$

where, R_d is photo detector responsivity, P_r is received optical power and N is the number of subcarriers. The optical r. m. s modulation index μ given by $\mu = m\sqrt{N/2}$ for a SCM system. σ_{th}^2 , σ_{shot}^2 , $\sigma_{intensity}^2$ and σ_x^2 represents the noise variance due to thermal noise, shot noise, relative intensity noise of laser and crosstalk respectively. Now putting the value of μ , equation (3.29) can be rewritten as-

$$CNR = \frac{(0.5mR_dP_r)^2}{\sigma_{th}^2 + \sigma_{shot}^2 + \sigma_{intensity}^2 + \sigma_x^2} \quad (3.30)$$

Once CNR is calculated, BER can be expressed as in [45],

$$BER = \frac{1}{2} \operatorname{erfc}\left(\frac{1}{2\sqrt{2}} \sqrt{CNR}\right) \quad (3.31)$$

where, erfc is the complementary error function.

3.7.1 Shot Noise

It arises from the statistical nature of the generation and collection of photoelectrons when an optical signal is incident on a photodiode. It was first studied by Schottky in 1918 and has been thoroughly investigated since then. The photo diode current generated in response to a constant optical signal can be written as [45], $I(t) = I_p + i_s(t)$ (3.31)

Where, $I_p = R_d P_{in}$ is the average current and $i_s(t)$ is the current fluctuation related to shot noise. Mathematically it is a stationary random process with Poission Statistics. The autocorrelation function of $i_s(t)$ is related to spectral density $S_s(f)$ by Wiener-Khinchin theorem [45]

$$\langle i_s(t)i_s(t+\tau) \rangle = \int_{-\infty}^{\infty} S_s(f) \exp(2\pi i f \tau) df \quad (3.32)$$

The spectral density of shot noise is constant and is given by $S_s(f) = eI_p$ (an example of white noise). Note that $S_s(f)$ is a two sided spectral density as negative frequencies are included in eq (3.32). If only the positive frequencies are considered by changing the lower limit of integration to zero, the one sided spectral density becomes $2eI_p$.

The noise variance is obtained by setting $\tau = 0$ in equation (3.32) as

$$\sigma_s^2 = \langle i_s^2(t) \rangle = \int_{-\infty}^{\infty} S_s(f) df = 2eI_p B \quad (3.33)$$

Where, B is the effective noise bandwidth of the receiver. The actual value of B depends on receiver design. Since dark current also generates shot noise equation (3.33) should rewrite as

$$\sigma_s^2 = 2e(I_p + I_d)B \quad (3.34)$$

The value σ_s is the rms value of noise current induced by shot noise.

3.7.2 Thermal Noise

At a finite temperature, electrons move randomly in any conductor. Random thermal motion of electrons in a resistor manifests current even at when there is no applied noise. The load resistance in front of an optical receiver adds such fluctuation to the current generated by the photodiode. This additional noise component is referred to as thermal noise. It is also called Johnson noise or Nyquist noise.

Thermal noise can be included by modifying equation (3.31) $I(t) = I_p + i_s(t) + i_T(t)$, where $i_T(t)$ is a current fluctuation induced by thermal noise. Mathematically $i_T(t)$ is modeled as Gaussian random process with a spectral density that is frequency independent up to $f \approx 1 \text{ THz}$ and is given by

$$S_T(f) = 2k_B T / R_L \quad (3.35)$$

where, k_B is the Boltzman constant, T is absolute temperature and R_L is the load resistance. As mentioned before $S_T(f)$ is the two sided spectral density.

The autocorrelation function of $i_T(t)$ is given by

$$\langle i_T(t)i_T(t+\tau) \rangle = \int_{-\infty}^{\infty} S_T(f) \exp(2\pi i f \tau) df \quad (3.36)$$

The noise variance can be found by substituting $\tau = 0$ in equation (3.36) and it becomes

$$\sigma_T^2 = \langle i_T^2(t) \rangle = \int_{-\infty}^{\infty} S_T(f) df = 4k_B T B / R_L \quad (3.37)$$

3.7.3 Relative Intensity noise

Fluctuation in intensity of the output from semiconductor laser also leads to optical intensity noise. The random intensity fluctuation created a noise source referred to as Relative Intensity Noise (RIN). It is defined as the ratio of mean square power fluctuation to the mean optical power squared which is emitted from the device ie

$$RIN = \frac{\overline{\delta P_O^2}}{(P_O)^2} \quad (3.38)$$

The above definition allows RIN to measure dB/Hz where the power fluctuation can be written as

$$\overline{\delta P_O^2} = \int_0^{\infty} S_{RIN}(f) df \quad (3.39)$$

Where, $S_{RIN}(f)$ is the power spectral density of RIN and related to $S_{RIN}(\omega)$ by

$$S_{RIN}(\omega) = 2\pi S_{RIN}(f) \quad (3.40)$$

RIN as a power fluctuation over a bandwidth B can be expressed as

$$RIN = \frac{S_{RIN}(f)B}{(P_O)^2} \quad (3.41)$$

Typically the RIN for a single mode semiconductor laser is in the range of 130 dB/Hz to 160 dB/Hz.

Hence the noise variance due to RIN can be expressed as

$$\sigma_{intensity}^2 = RIN(R_d P_O)^2 B \quad (3.42)$$

3.7.4 Signal Crosstalk Noise Term

In presence of crosstalk the detected photo current can be written following [32] and [40] as:

$$I_p = R_d \{P_S + P_X + 2\sqrt{P_S P_X} \cos(\Delta\theta)\} + i_{shot} + i_{thermal} + i_{intensity} \quad (3.43)$$

Where, P_S and P_X are the optical channel power of signal and crosstalk power respectively. The detectable power comprises the signal power from first term, the crosstalk from second term and additional term due to interaction between two fields.

Assuming $P_S \gg P_X$ equation (3.43) can be rewritten as

$$I_p = R_d \{P_S + i_X\} + i_{shot} + i_{thermal} + i_{intensity} \quad (3.44)$$

$$i_X = 2\sqrt{P_S P_X} \cos(\Delta\theta)$$

using Gaussian approximation the signal crosstalk noise variance can be written as in [32]:

$$\langle i_X \rangle = 0$$

$$\sigma_X^2 = \langle i_X^2 \rangle - \langle i_X \rangle^2$$

$$= 4R_d^2 P_S P_X \cos^2(\Delta\theta)$$

$$= 2R_d^2 P_S P_X$$

$$= 2I_S^2 X$$

$$(3.45)$$

Where, X is the ratio of crosstalk optical power to the signal optical power.

CHAPTER-4

RESULTS AND DISCUSSIONS

Following the theoretical analysis presented in chapter 3, theoretical performance results of SCM-WDM transmission system are evaluated with and without considering fiber nonlinear effects. First SRS, XPM and FWM induced crosstalks are analyzed individually and then their combined effects are evaluated. The parameters used in theoretical computations are given in Table 4.1 (unless stated in discussion).

Table 4.1
Parameter values use for theoretical calculations

Parameter	Value
RF Subcarrier freq., ω	varied
Launch power on λ_j , P_j	varied
Raman gain between λ_i & λ_j , g_{ij}	Ref. [24]
Fibre length, L	25 km
Fibre loss, α	0.21 dB/Km
Dispersion Coefficient, D (SMF)	17 ps/nm/km
Dispersion Coefficient, D (SMF)	2 ps/nm/km
Mode effective area, A_{eff} (SMF)	80 μm^2
Mode effective area, A_{eff} (DSF)	55 μm^2
Nonlinear refractive index, n_2	$2.65 \times 10^{-20} \text{ m}^2/\text{W}$
Speed of light, c	$2.998 \times 10^8 \text{ m/s}^2$
Wavelength channel spacing	1 nm
Optical modulation index, m	4%
Capacity per Wavelength channel	10 Gb/s
Number of subcarriers per WDM channel	50

4.1 EFFECT OF XPM INDUCED CROSSTALK

Consider a three channel WDM system with average input power per channel 10 dBm.

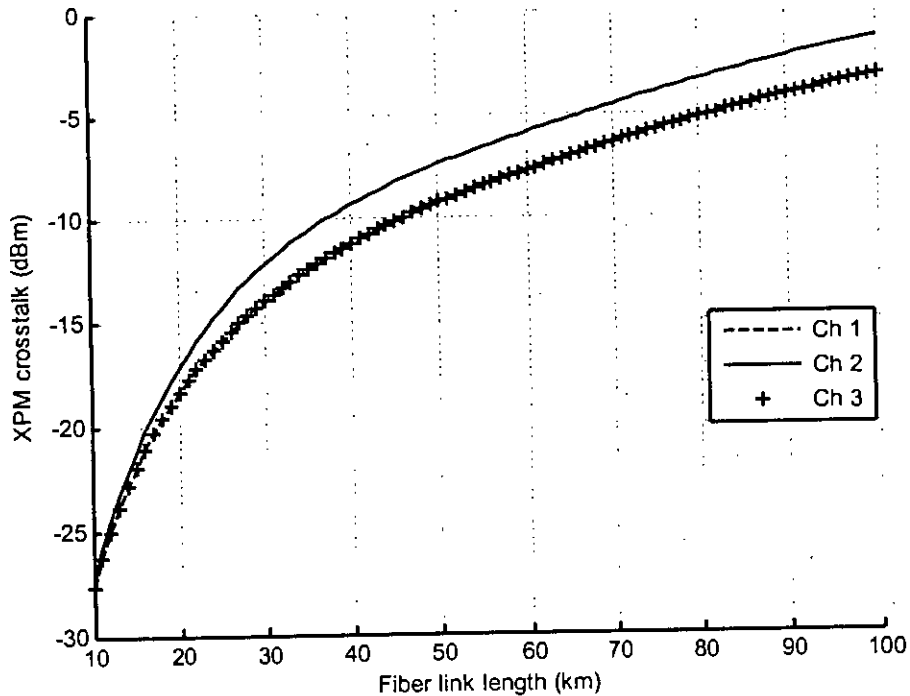


Fig. 4.1: XPM crosstalk level in three WDM channels with varying fiber link length for $\Delta\lambda=1$ nm, $f = 1$ GHz & $P_{in} = 10$ dBm.

Fig. 4.1 shows the theoretical crosstalk level in three different WDM channels with varying fiber link length for $\Delta\lambda=1$ nm, $f = 1$ GHz. The magnitudes of crosstalk in 1st and 3rd channel are equal as same power and assumed in each WDM channel and equal channel spacing is considered. Central channel suffers from most crosstalk since it is most affected by the interaction of various channels. Henceforth, the XPM crosstalk analysis is limited to investigations of central channel only. It is also observed from the figure that as the optical link length increases, crosstalk also increases as the interactions among the channels increase.

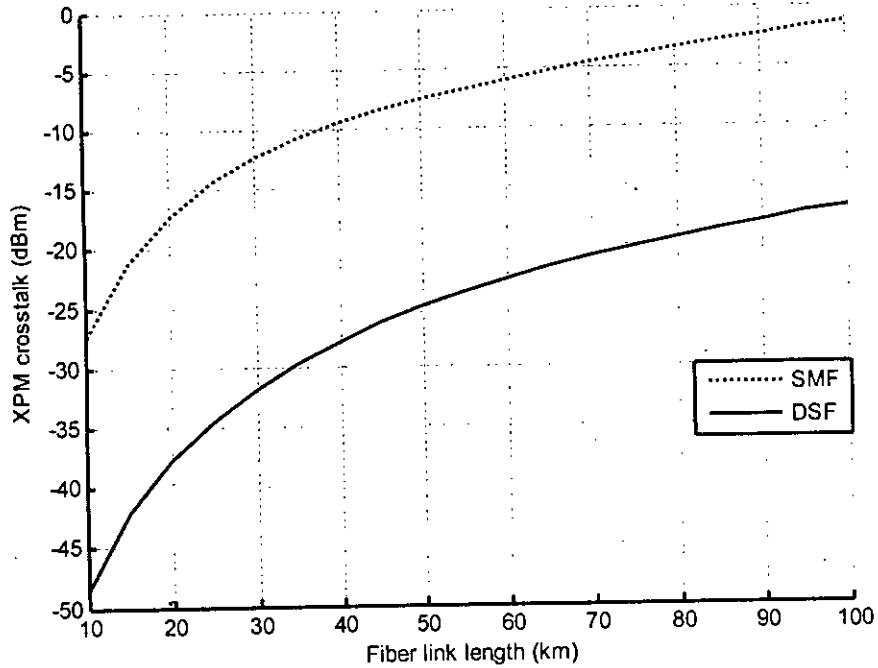


Fig.4.2: XPM crosstalk with varying link length for DSF and SMF for $\Delta\lambda = 1$ nm, $P_{in}=10$ dBm and $f = 1$ GHz.

Fig.4.2 shows the XPM crosstalk level in central channel (worst case) with varying link length for $\Delta\lambda = 1$ nm and $f = 1$ GHz for both DSF and SMF. Without dispersion phase modulation (PM) due to XPM can not be converted to intensity modulation (IM). Since DSF has low chromatic dispersion, crosstalk induced by XPM is much less in DSF than standard SMF. For example, as shown in Fig.4.2, for a launch power of 10 dBm per channel crosstalk at fiber link length at 25 km is -35 dBm for DSF. For same conditions crosstalk is -15 dBm for SMF. Hence further analysis of XPM induced crosstalk is limited for SMF.

Fig.4.3 shows the XPM crosstalk level in central channel (worst case) with varying link length for different wavelength for $f = 1.0$ GHz, $M=3$ and $P_{in} = 10$ dBm. It is clear that crosstalk increases with decreasing channel spacing as walk-off parameter is less for dense wavelength channel spacing. It is further noticed from the figure that for a short link length effect of channel spacing is less while its effect increases with increasing link length.

Fig.4.4 further confirm the effect of channel spacing on XPM crosstalk level. It is clear from the figure that crosstalk decreases a considerable amount with increasing $\Delta\lambda$.

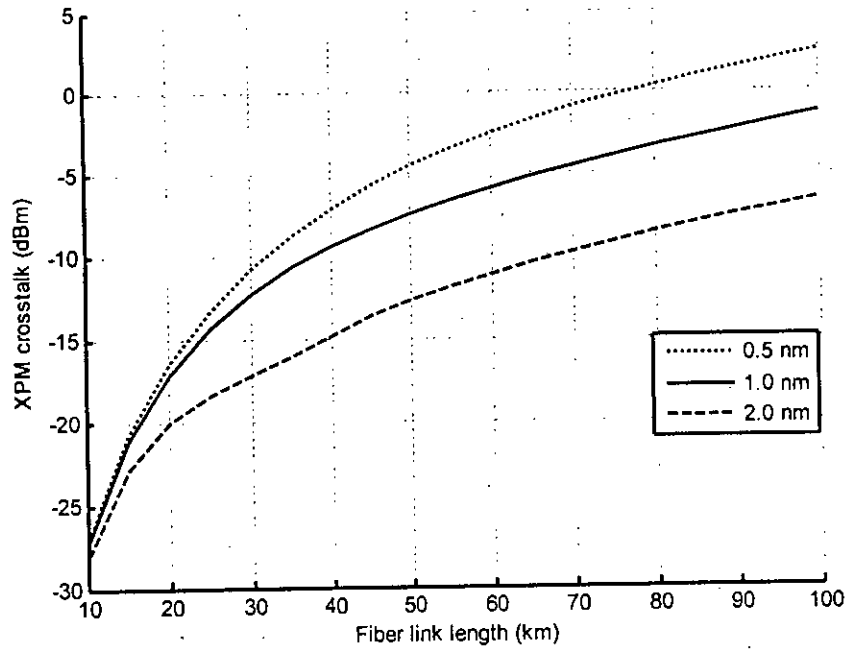


Fig.4.3: XPM induced crosstalk with varying link length for different wavelength channel spacing for $P_{in}=10\text{dBm}$, $f = 1\text{GHz}$ and $M=3$.

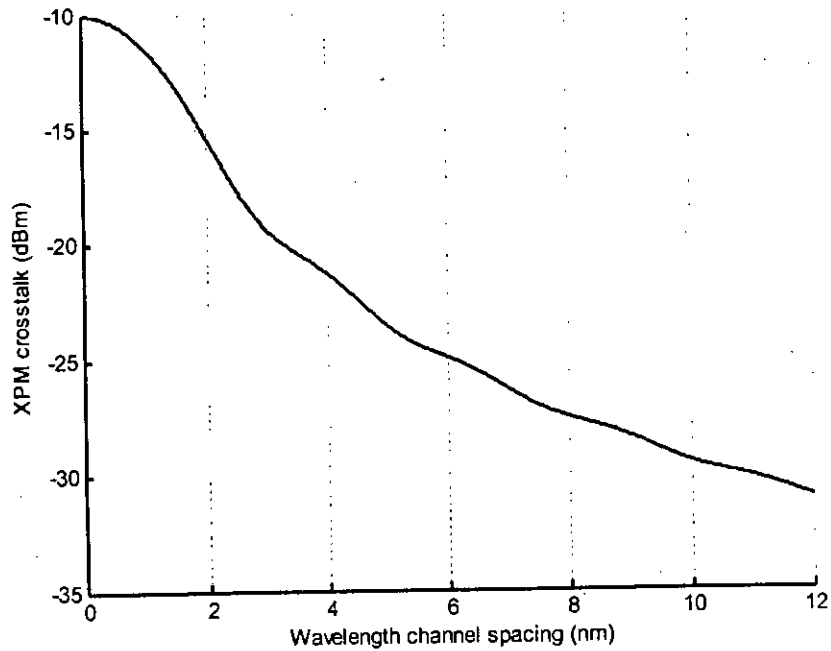


Fig.4.4: XPM induced crosstalk in central channel vs channel spacing for $L = 25\text{ km}$, $M=3$, $f=1\text{ GHz}$ and $P_{in} = 10\text{ dBm}$

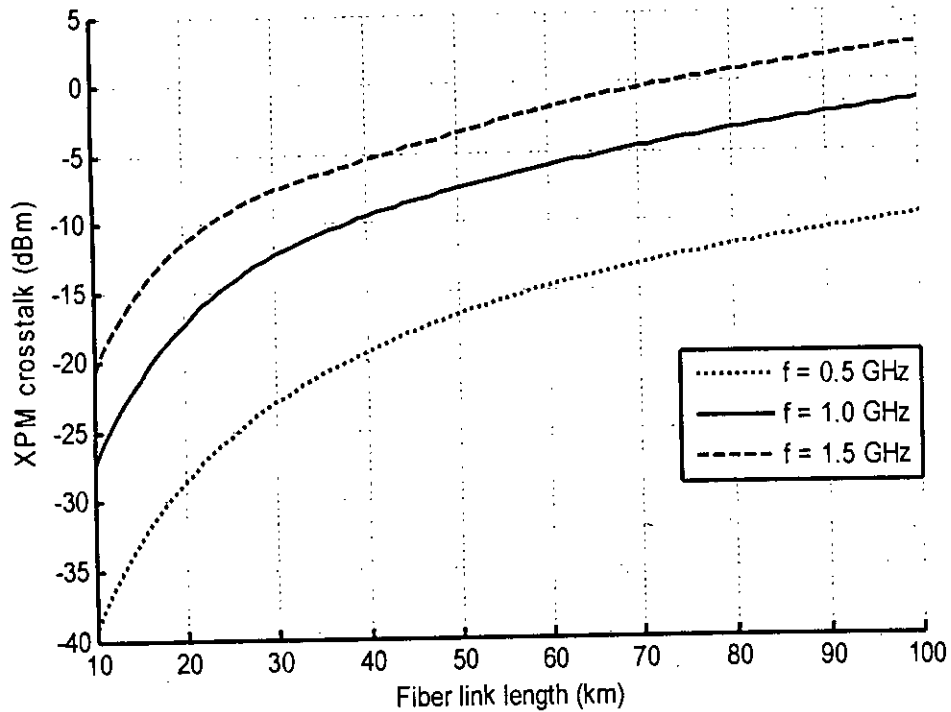


Fig.4.5 XPM induced crosstalk in central channel with varying link length for different modulation frequency for $\Delta\lambda = 1$ nm, $M=3$ and $P_{in} = 10$ dBm

Fig.4.5 shows the effect of modulation frequency on XPM induced crosstalk with varying link length. It is found that crosstalk increases with increasing modulation frequency. For example, at 25 km fiber link length with $\Delta\lambda = 1$ nm, $M=3$ and $P_{in} = 10$ dBm crosstalk level at central wavelength channel for 0.5 GHz, 1.0 GHz and 1.5 GHz modulation frequencies are -25 dBm, -14 dBm and -9 dBm respectively.

XPM crosstalk level with varying modulation is further illustrated for fiber link length of 25 km, 50 km, 75 km and 100 km in the Fig.4.6. XPM induced crosstalk actually grows with ω^2 and it is clear from Fig.4.6 crosstalk is dominant at higher modulation frequencies.

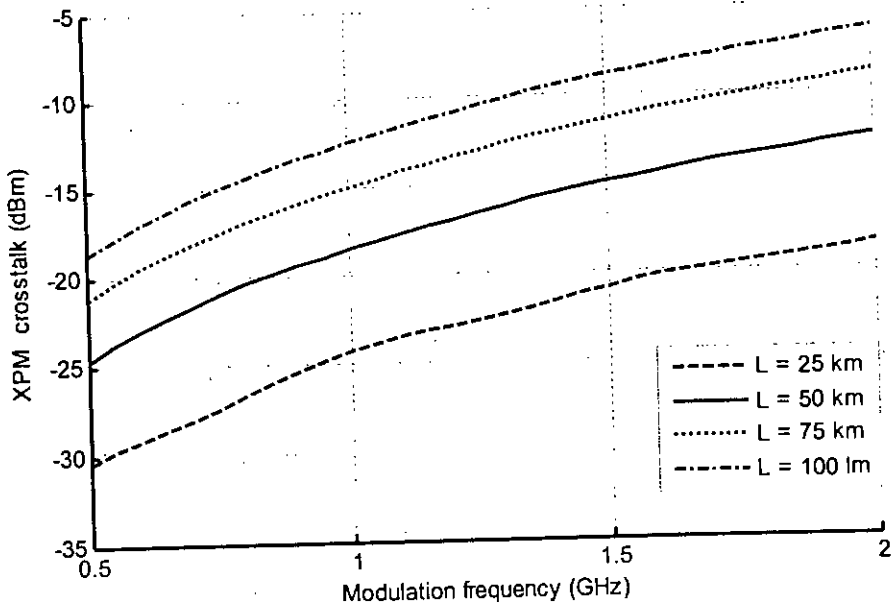


Fig.4.6: XPM induced crosstalk in central channel with varying modulation frequency for different fiber link length for $\Delta\lambda = 1$ nm, $M=3$ and $P_{in}= 10$ dBm.

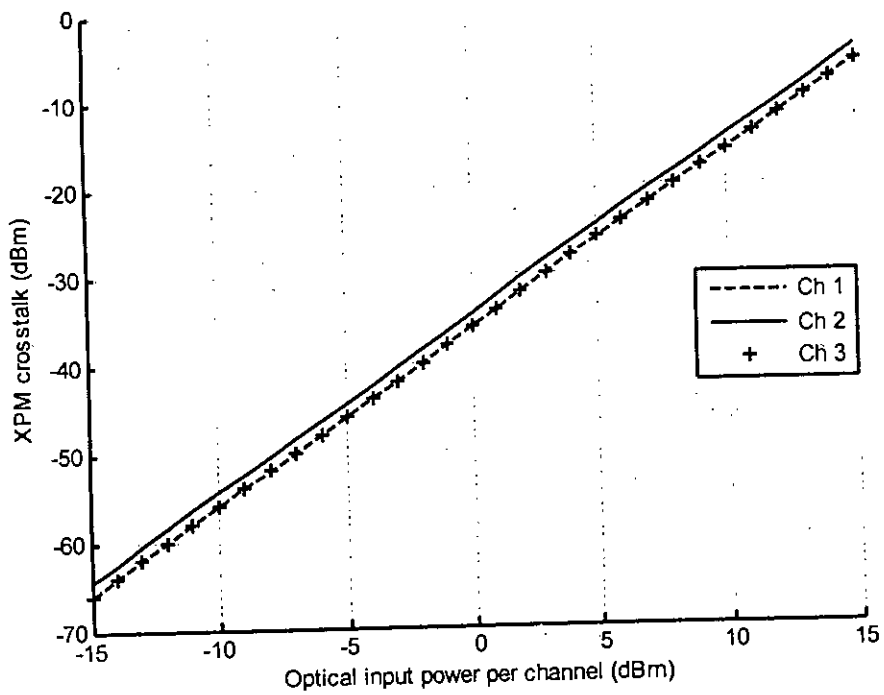


Fig.4.7: XPM induced crosstalk in different channel with varying optical power per wavelength channel for $\Delta\lambda = 1$ nm, $L = 25$ km, $M=3$ and $f = 1$ GHz.

It is found from Fig.4.7 that XPM induced crosstalk increases linearly with increasing optical launch power per wavelength channel as it shown in theoretical analysis that XPM crosstalk is a factor of P_{in} .

Fig.4.8 shows the XPM crosstalk level in central channel with varying number of WDM channel for $L = 25$, $\Delta\lambda=1$ nm, $P_{in} = 10$ dBm and $f = 1$ GHz. It is found that crosstalk does not increase linearly, because for a given channel spacing, central channel suffers strong crosstalk from adjacent channels but less crosstalk from far channels.

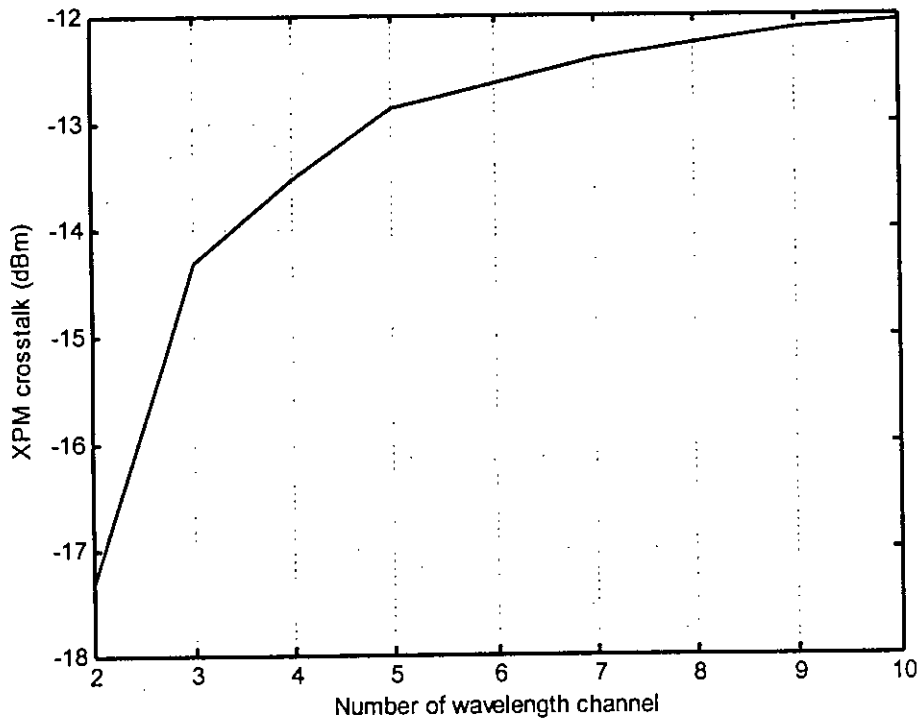


Fig.4.8: XPM crosstalk level in central channel with varying number of WDM channel for $L = 25$, $\Delta\lambda=1$ nm, $P_{in} = 10$ dBm and $f = 1$ GHz

Hence the characteristics of XPM crosstalk can be summarized as below:

1. As wavelength separation decreases, XPM crosstalk increases.
2. XPM crosstalk dominants at large modulation frequency.
3. Low dispersive fiber suffers less XPM crosstalk.
4. XPM increases with increasing fiber link length.

4.2 EFFECT OF SRS INDUCED CROSSTALK

For the analysis of SRS induced crosstalk in SCM-WDM system, we consider three wavelength channels such that $\lambda_1 < \lambda_2 < \lambda_3$ with an equal channel spacing and an equal power is consider for each wavelength channel. As mentioned in the theory, crosstalk due to SRS in central channel will be zero (unlike XPM crosstalk where this channel suffers the highest crosstalk). The magnitude of power depletion in lowest wavelength channel (Ch - 1) is same as the crosstalk in highest wavelength channel (Ch - 3). This is due to same walk - off effect and same magnitude of Raman gain.

Fig.4.9 shows the crosstalk level of highest wavelength channel of a three channel WDM system due to SRS with varying link length for different modulation frequency for $\Delta\lambda = 1$ nm and $P_{in} = 10$ dBm. It is clear from the figure that unlike XPM, SRS crosstalk decreases with increasing modulation frequency. But crosstalk level is essentially constant for any link length.

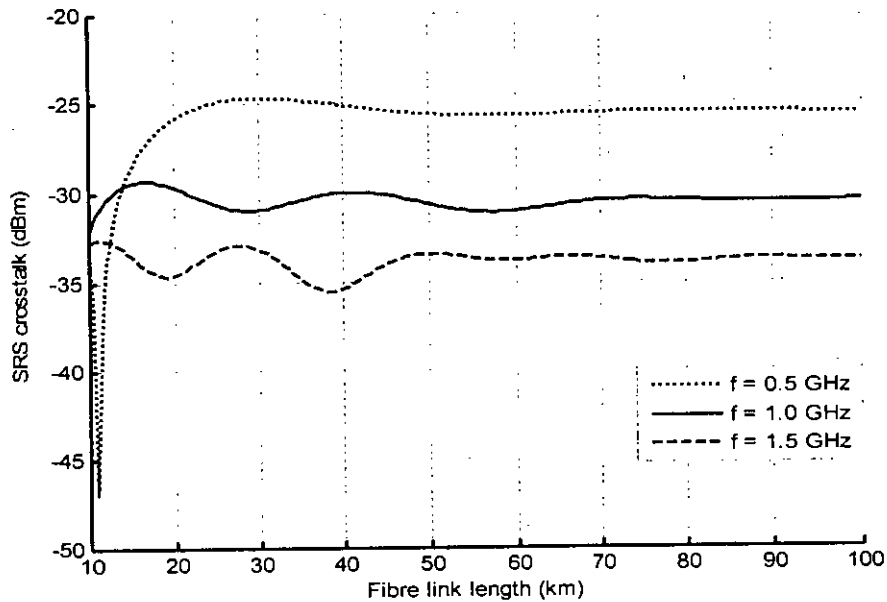


Fig.4.9: SRS induced crosstalk in λ_3 channel with varying link length at different modulation frequency for $\Delta\lambda = 1$ nm and $P_{in}=10$ dBm

Effect of modulation frequency is further confirmed in Fig.4.10 where SRS crosstalk level is plotted against modulation frequency for a channel spacing of 1 nm. An inverse characteristic is found for SRS crosstalk and modulation frequency.

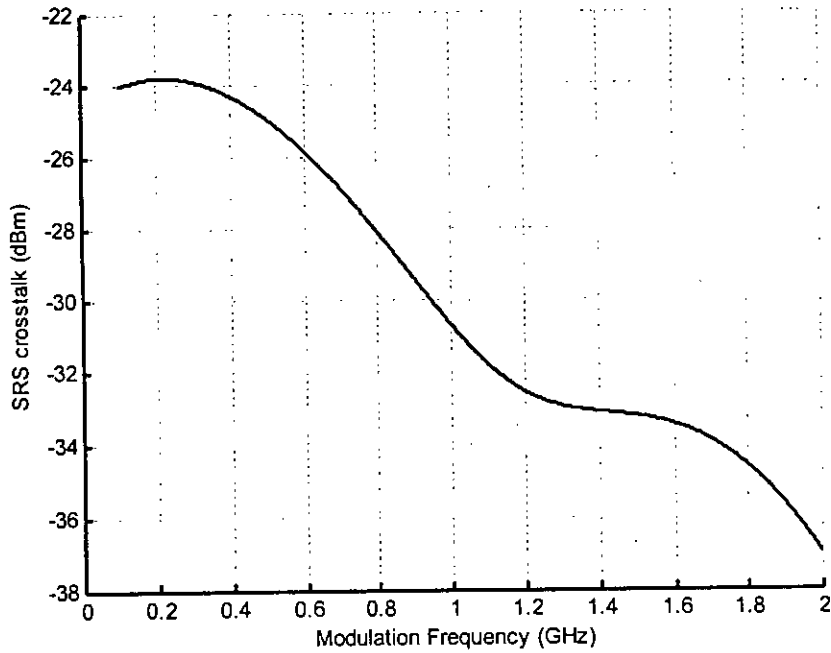


Fig.4.10: SRS induced crosstalk in λ_3 channel with varying modulation frequency for $L=25$ km, $\Delta\lambda = 1$ nm and $P_{in}=10$ dBm

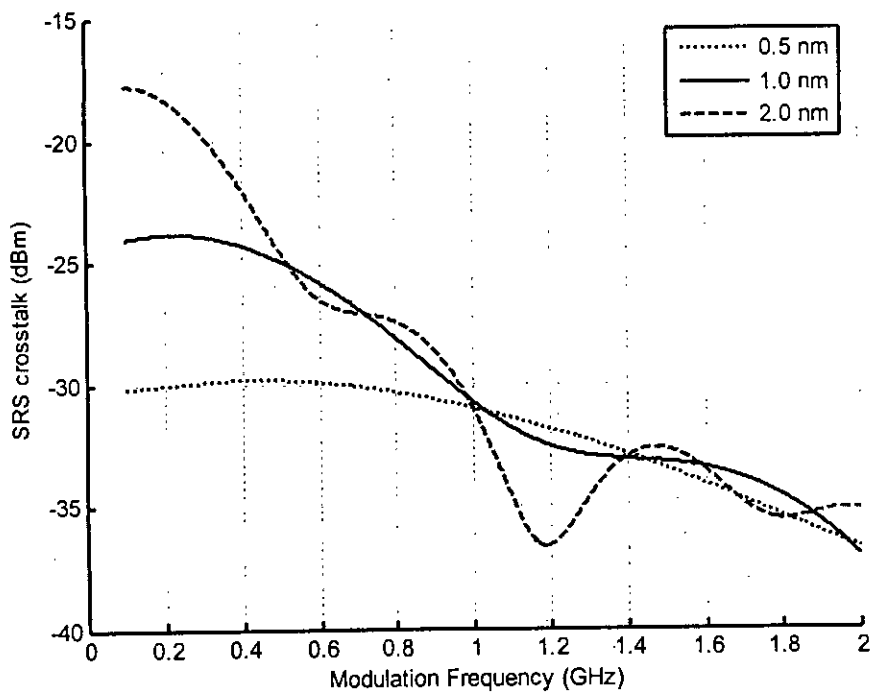


Fig.4.11: SRS induced crosstalk in λ_3 channel with varying modulation frequency at different channel spacing for $L=25$ km, and $P_{in}=10$ dBm

To demonstrate the effect of wavelength channel spacing consider SRS induced crosstalk in λ_3 channel is plotted against modulation frequency at different channel spacing for $L=25$ km, and $P_{in}=10$ dBm in Fig.4.11. It is observed that SRS induced crosstalk level is high for large channel spacing at low modulation frequency. For example, for the above mentioned conditions below 500 MHz modulation frequency, crosstalk level is dominant at large channel spacing but approximately constant for all wavelength separation at higher frequency.

To illustrate the effect of channel spacing more clearly SRS induced crosstalk is plotted with varying fiber link length at a low modulation frequency (400 MHz). Same result is found again, higher crosstalk for higher channel spacing.

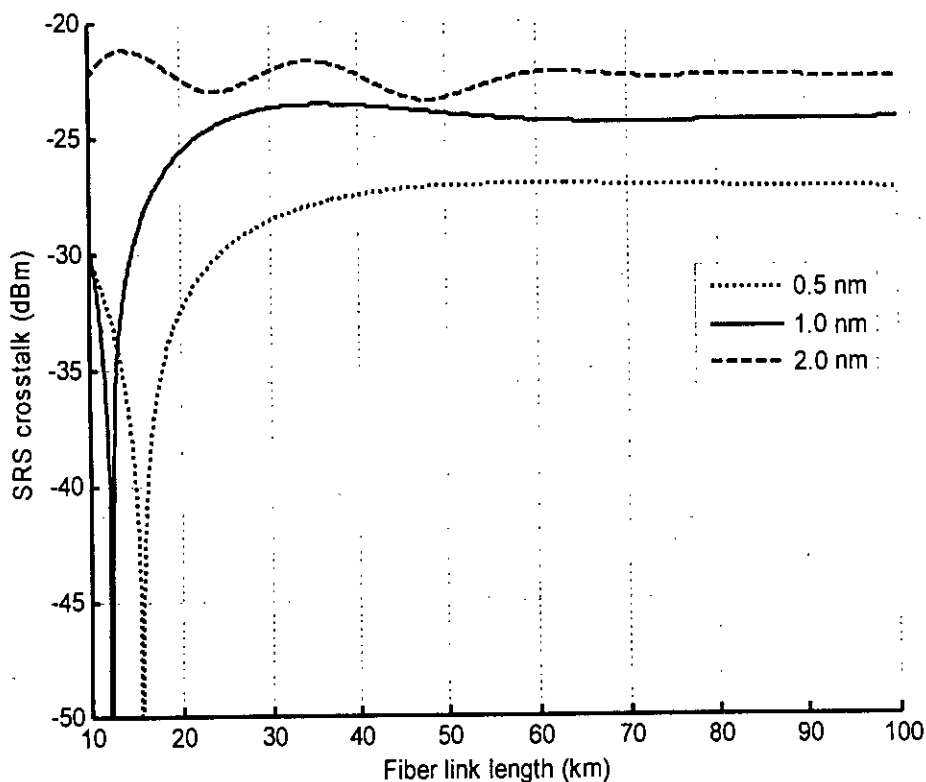


Fig.4.12: SRS induced crosstalk in λ_3 channel with varying link length at different channel spacing for $f=0.4$ GHz, and $P_{in}=10$ dBm

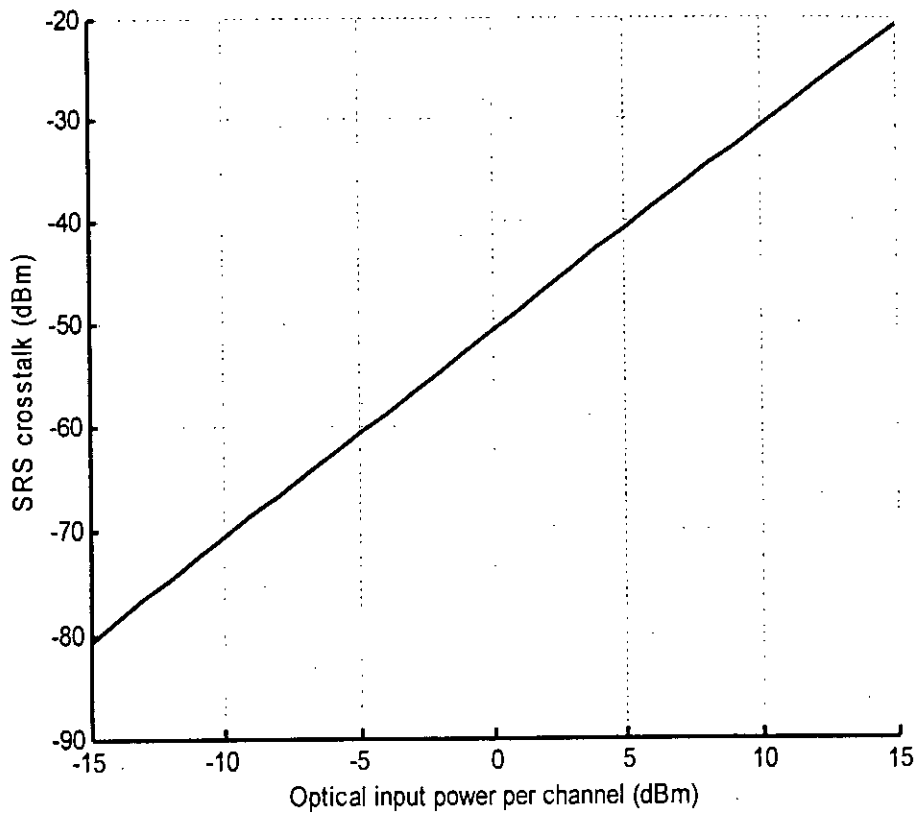


Fig.4.13: SRS induced crosstalk in λ_3 channel with varying optical launch power per WDM channel for $L=25$ km, $\Delta\lambda=1$ nm, and $f= 1.0$ GHz.

It is found from Fig.4.13 that XPM induced crosstalk increases linearly with increasing optical launch power per wavelength channel as it shown in theoretical analysis that SRS crosstalk is a factor of P_{in} .

Fig.4.14 shows the SRS crosstalk level in highest wavelength channel with varying number of WDM channel for $L = 25$, $\Delta\lambda=1$ nm, $P_{in} = 10$ dBm and $f= 1$ GHz. It is found that crosstalk increases approximately linearly, because unlike XPM, crosstalk from far channels can not be neglected while considering SRS crosstalk.

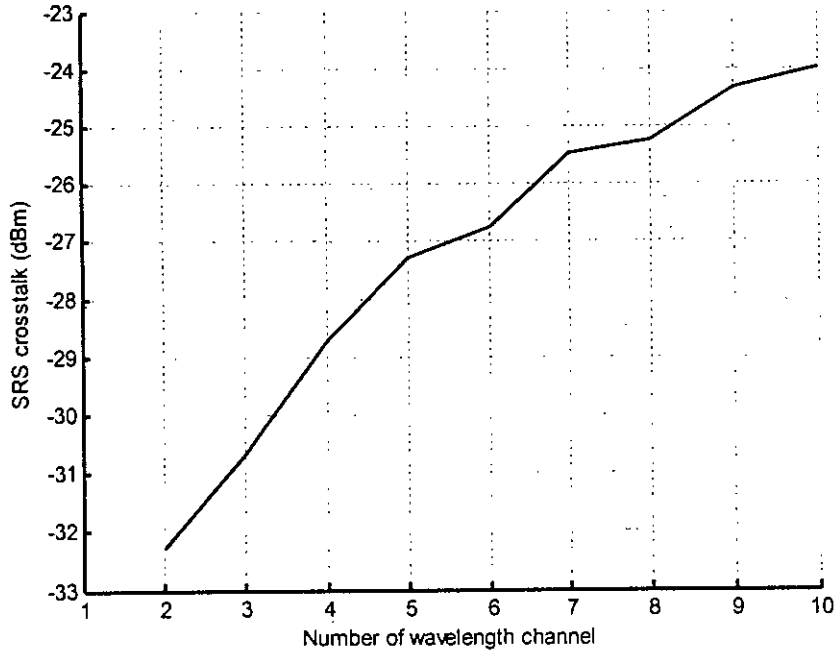


Fig.4.14: SRS crosstalk level in central channel with varying number of wavelength channel for $L = 25$, $\Delta\lambda=1$ nm, $P_{in} = 10$ dBm and $f= 1$ GHz

Hence, the characteristics of SRS crosstalk can be summarized as below:

1. Crosstalk is dominant at lower modulation frequency.
2. Up to certain modulation frequency (500 MHz), crosstalk increases with increasing channel spacing.
3. SRS crosstalk is essentially constant for all fiber link length.

4.3 COMBINED EFFECT OF SRS & XPM CROSSTALK

Based on constructive and destructive SRS+XPM theory discussed in chapter 3, this section analyzes the effect of combine effect of SRS and XPM crosstalk. As mentioned earlier SRS crosstalk is dominant at highest wavelength channel while XPM crosstalk in central channel. So, it is an interesting issue to find the worst channel in presence of both SRS and XPM induced crosstalk.

Fig.4.15 shows crosstalk level due to combined influence of SRS & XPM in three different channels with varying link length for $P_{in}=10\text{dBm}$, $f=0.5\text{ GHz}$ and $\Delta\lambda=3\text{nm}$. From the figure it is found that up to 65 km 3rd channel (highest wavelength) suffers more crosstalk than 2nd channel (central channel) due to higher channel spacing and low modulation frequency.

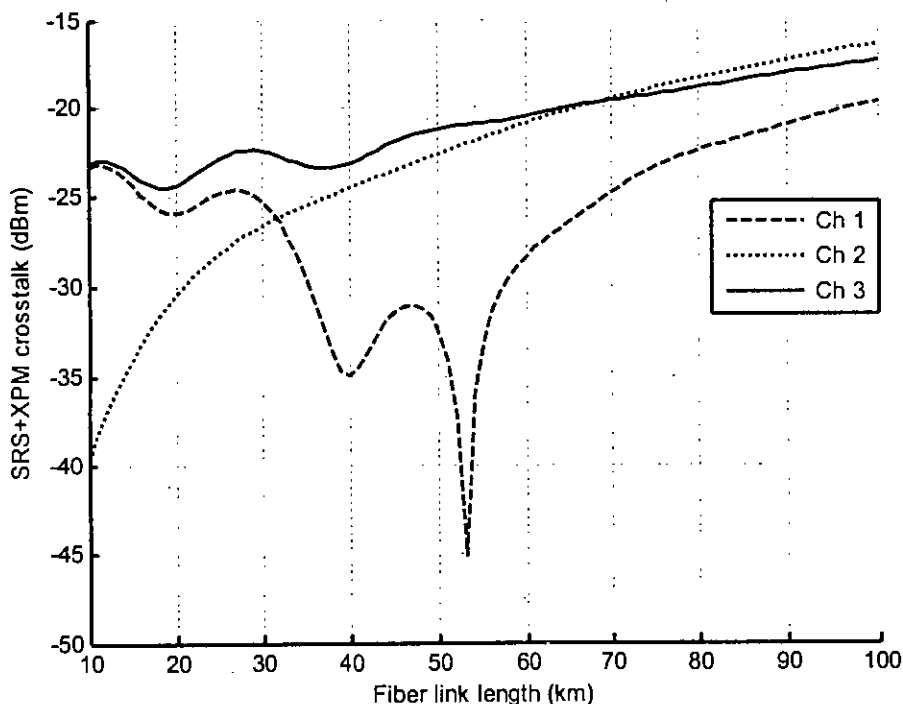


Fig.4.15: Combined crosstalk due to SRS & XPM in three different channels with varying link length for $P_{in}=10\text{dBm}$, $f=0.5\text{ GHz}$ and $\Delta\lambda=3\text{nm}$.

If channel spacing is reduced to 1 nm then XPM crosstalk increases while SRS crosstalk decreases. In that case 3rd channel suffers more crosstalk than 2nd channel up to 40 km which is shown in Fig.4.16.

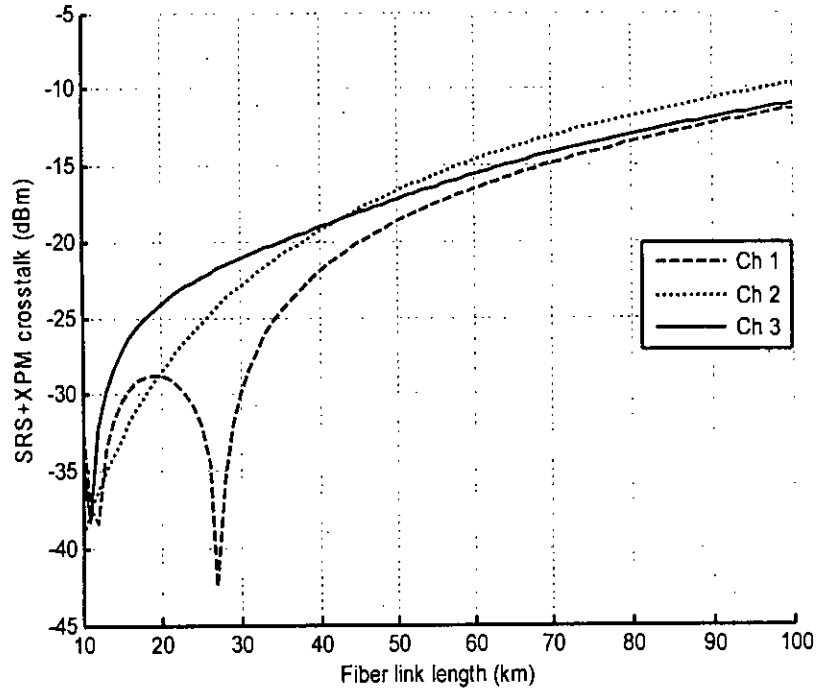


Fig.4.16: Combined crosstalk due to SRS & XPM in three different channels with varying link length for $P_{in}=10\text{dBm}$, $f= 0.5 \text{ GHz}$ and $\Delta\lambda=1\text{nm}$.

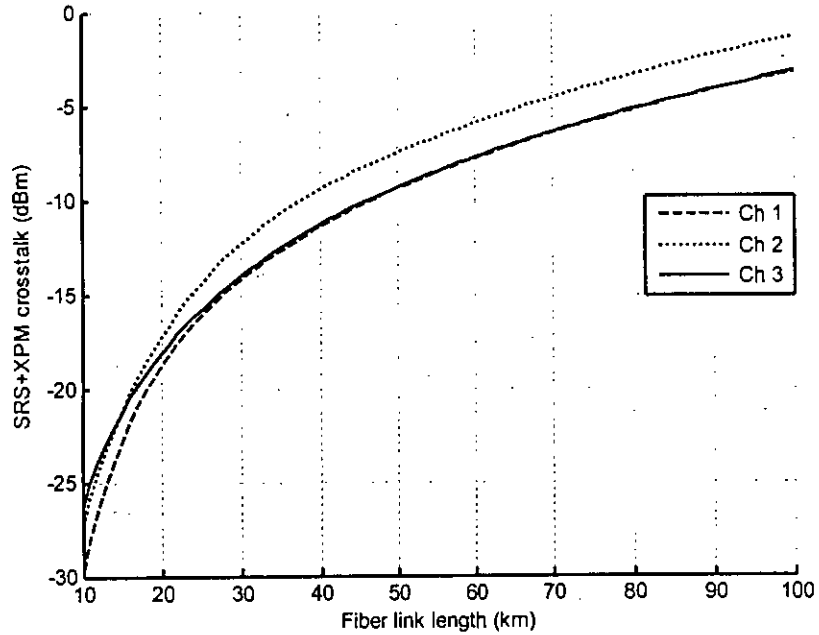


Fig4.17: Combined crosstalk due to SRS & XPM in three different channels with varying link length for $P_{in}=10\text{dBm}$, $f= 1.0 \text{ GHz}$ and $\Delta\lambda=1\text{nm}$.

Now, if modulation frequency is increased to 1 GHz, SRS crosstalk further decreases while XPM crosstalk increases. Hence the combined crosstalk is dominated by XPM and 2nd channel suffers crosstalk mostly even at low fiber length as 12 km.

Hence it can be concluded that highest wavelength channel suffers mostly by combined crosstalk due to SRS & XPM for low modulation frequency, short link length and higher channel spacing. Central channel suffers mostly in the contradictory conditions ie high modulation frequency, long link length and dense channel spacing.

4.4 EFFECT OF FWM INDUCED CROSSTALK

FWM efficiency decreases with increasing channel spacing, chromatic dispersion or transmission length due to increased phase mismatch between the signals. Fig.4.18 shows the FWM efficiency with varying channel spacing for both DSF and SMF for $L=25$ km. It is noted from the figure that FWM efficiency is high only at low channel spacing. With large chromatic dispersion, for example, signals of 1550 nm propagating through a conventional SMF mixing efficiency drops beyond 0.2 nm channel spacing while for DSF this value is 0.5 nm. Therefore, the effect of FWM may be significantly stronger when conventional fibers are used with 1330 nm sources or when dispersion shifted fibers are used with 1550 nm sources.

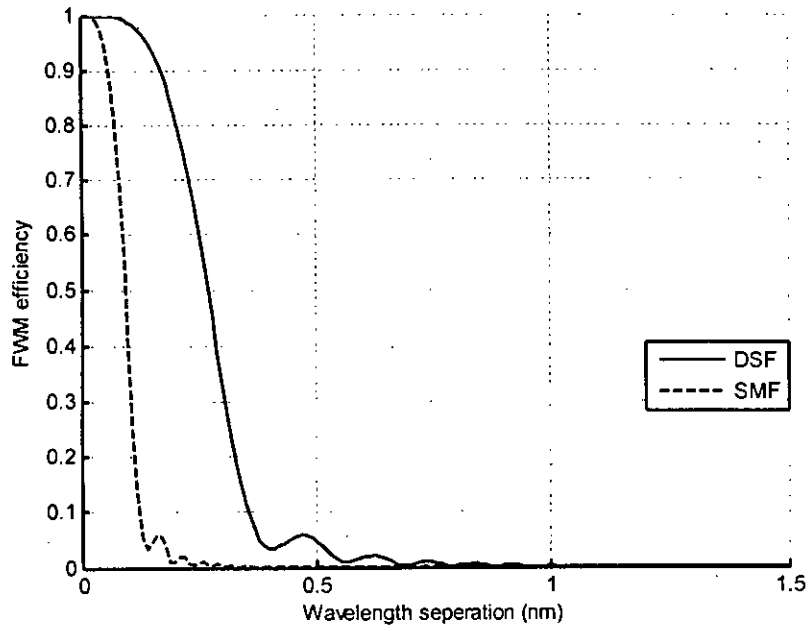


Fig.4.18: FWM efficiency vs wavelength channel spacing for DSF and SMF for $L=25$ km.

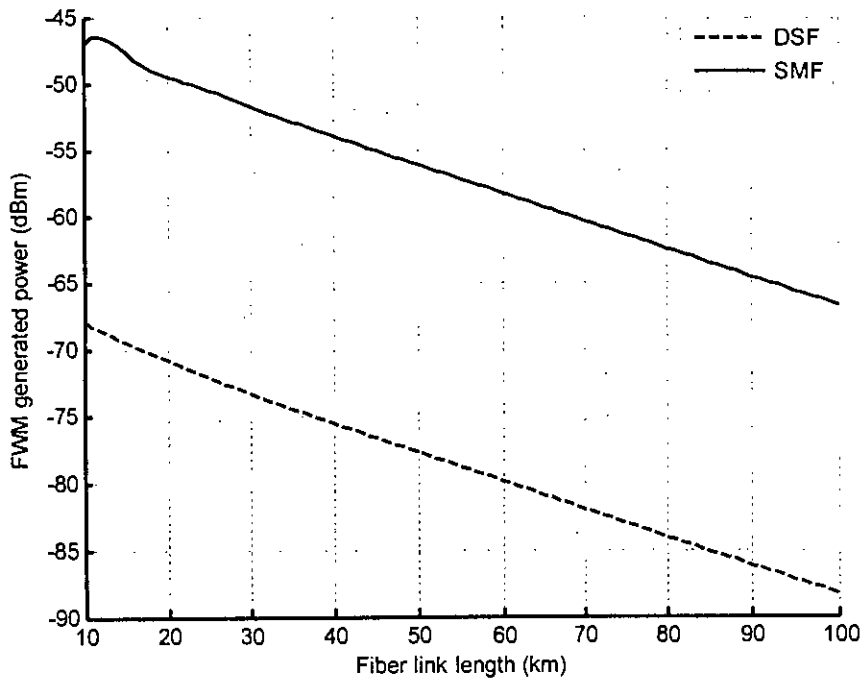


Fig.4.19: FWM induced crosstalk with varying link length for $M=3$, $N=50$, $P_{in}=0$ dBm and $\Delta\lambda = 0.5$ nm.

Fig.4.19 shows the effect of FWM crosstalk as a function of fiber link length for $M=3$, $N=50$, $P_{in}=0$ dBm and $\Delta\lambda = 0.5$ nm. Since FWM power is generated due to launch power to fiber input, FWM crosstalk decreases with increasing fiber link length due to fiber attenuation. It is also found from the figure that for a link length 25 km FWM crosstalk is -52.5 dBm for SMF and it is increased to -32 dBm for DSF. Since DSF has higher crosstalk level than SMF, further analysis is limited to DSF only.

Effect of number of WDM channel on crosstalk is shown in Fig.4.20. The figure shows the crosstalk level as a function number of subcarriers per channel with different values of M for $\Delta\lambda=0.5$ nm, $P_{in}=0$ dBm, $L=25$ km in a dispersion shifted fiber. Crosstalk increases sharply with increasing M values as the FWM generating terms increases largely with increasing M . In this example system, crosstalks for 50 subcarriers per channel are -50.2 dBm, -46.2 dBm and -43.8 dBm for 3, 4 and 5 wavelength channels respectively.

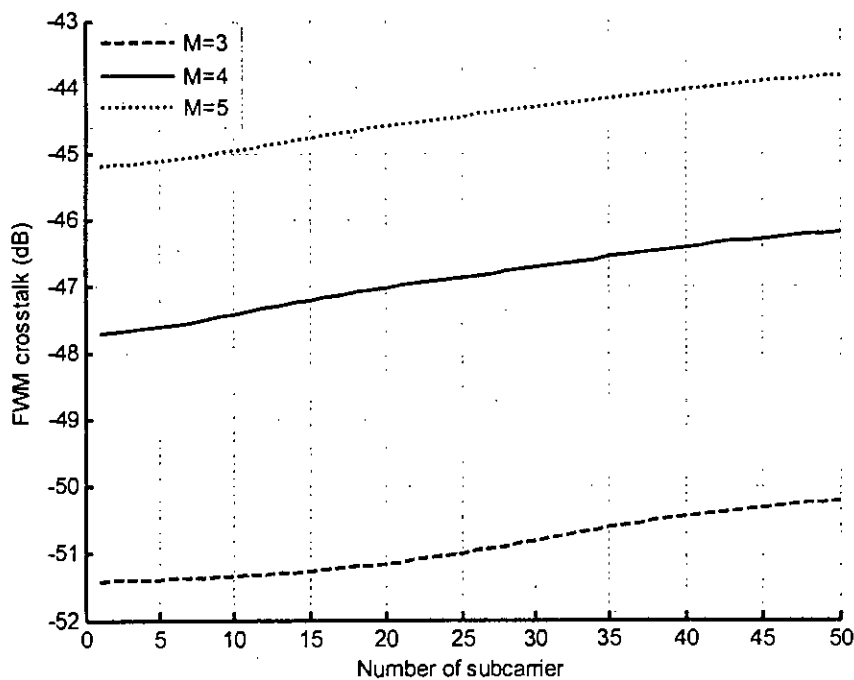


Fig.4.20: FWM induced crosstalk vs number of subcarriers per λ channel for different number of wavelength channel for $P_{in}=0$ dBm, $\Delta\lambda= 0.5$ nm and $L=25$ km.

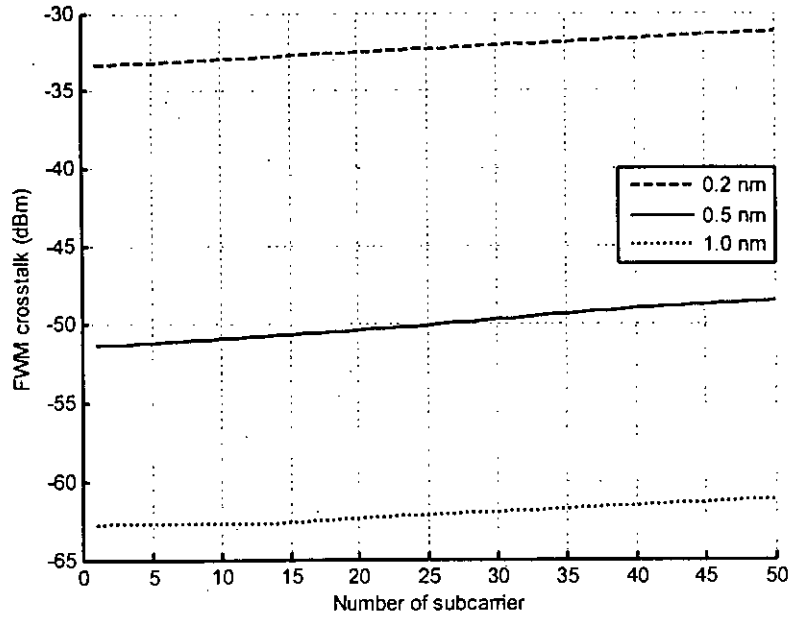


Fig.4.21: FWM induced crosstalk vs number of subcarriers per λ channel for different number of wavelength channel for $P_{in}=0$ dBm, $M=3$ and $L=25$ km.

Fig.4.21 illustrates the effect of wavelength separation with varying number of subcarriers per WDM channel for $P_{in}=0$ dBm, $M=3$ and $L=25$ km for a DSF. FWM crosstalk increases with decreasing channel spacing as it is predicted from FWM efficiency curve in Fig.4.16. For example, for 50 subcarriers per WDM channel crosstalk level is -32 dBm for 0.2 nm spacing, -48 dBm for 0.5 nm spacing and it further decreases to only -62 dBm for 1 nm spacing.

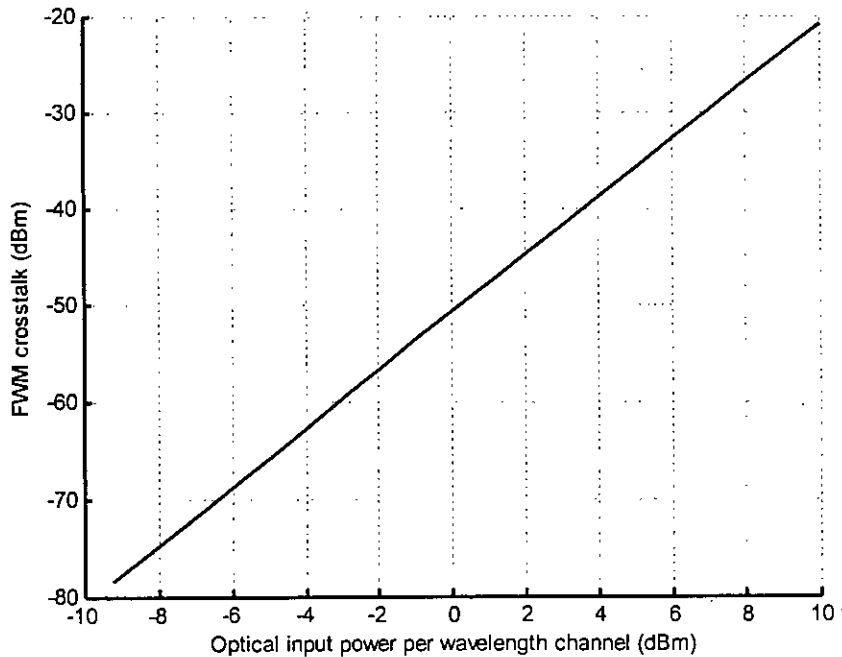


Fig.4.22: FWM crosstalk with varying optical power per WDM channel for $\Delta\lambda = 0.5$ nm, $L=25$, $M=3$, $N=50$.

Fig.4.22 shows the FWM induced crosstalk level with varying optical channel per λ channel for $\Delta\lambda = 0.5$ nm, $L=25$, $M=3$, $N=50$ for a DSF. It is found that crosstalk increases linearly with input launch power as FWM crosstalk increases as a factor of P_{in}^3 .

Hence FWM crosstalk characteristics can be summarized as below:

1. FWM induced crosstalk is dominant at low dispersive fiber.
2. For dense wavelength separation (less than 0.5 nm) FWM crosstalk is strong.
3. FWM crosstalk increases with increasing number of subcarriers and largely with increasing number of wavelength channel.

4.5 PERFORMANCE ANALYSIS USING SMF

From the crosstalk analysis in the previous section, it is clear that in dispersive fiber and dense wavelength spacing FWM is the dominating crosstalk source while in standard SMF, XPM and SRS is the major crosstalk contributing phenomena. So, while performing analysis in DSF fiber FWM crosstalk is counted and combined influence of SRS and XPM is considered in SMF.

Fig.4.23 shows the variation of BER of the system with varying optical input power per channel for different values of link length at bit rate =10 Gb/s, receiver sensitivity = -14dBm, $M=3$, $N=50$, $\Delta\lambda=1$ nm. As link length increases, due to phase modulation of a signal increases and with fiber chromatic dispersion it converts to intensity modulation, thus an increased crosstalk. So, less optical power is allowed to launch to fiber input with long distance system.

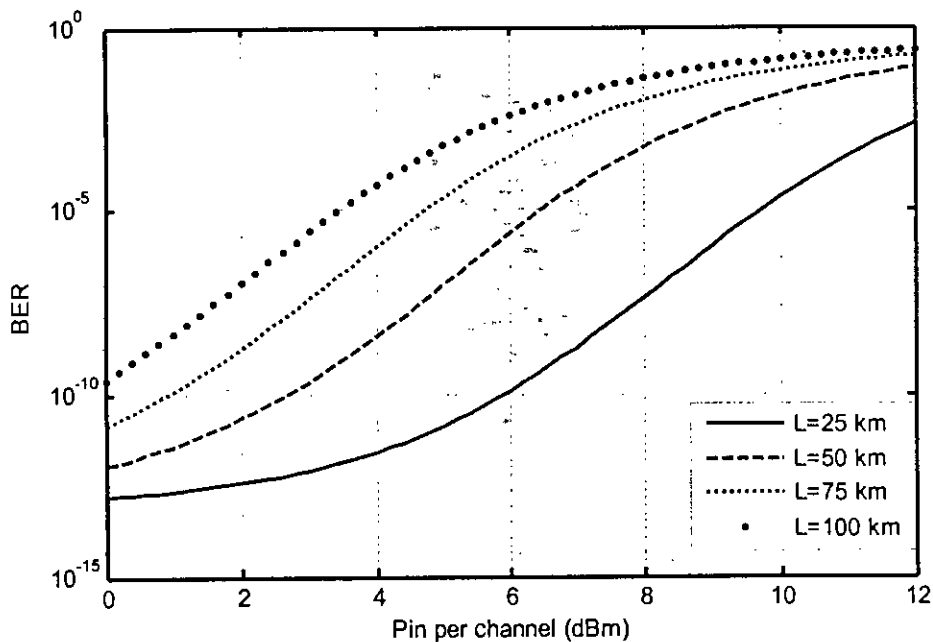


Fig.4.23: BER as a function of optical input power per channel for different link length at bit rate =10 Gb/s, receiver sensitivity = -14dBm, $M=3$, $N=50$, $\Delta\lambda=1$ nm.

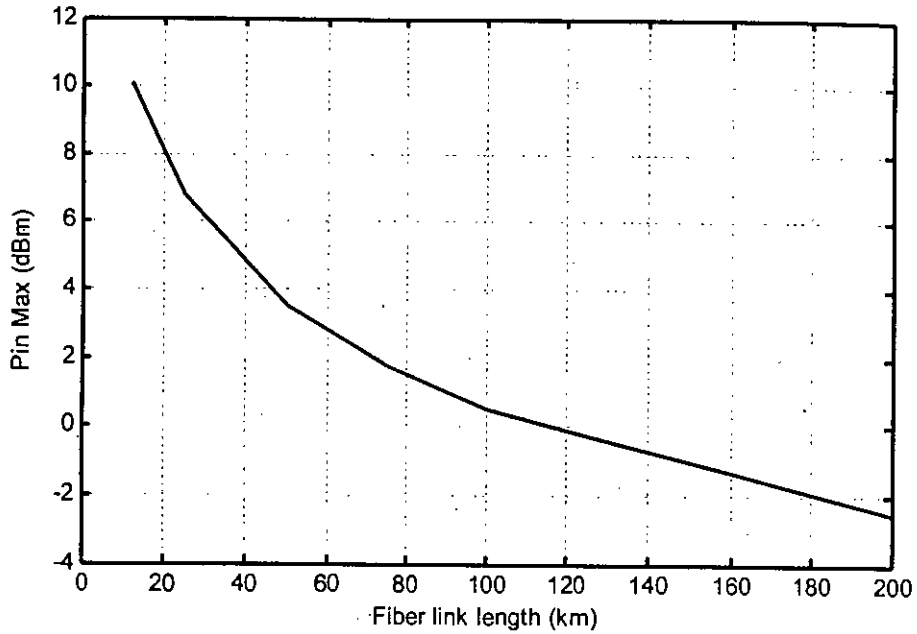


Fig.4.24: Maximum allowable optical input power at BER of 10^{-9} with varying fiber link length at bit rate =10 Gb/s, $M=3$, $N=50$, $\Delta\lambda=1.0$ nm & receiver sen.= -14 dBm.

To investigate the allowable launch optical power per channel, received power is kept constant which can be done by using an attenuator in the receiver.

Fig. 4.24 shows maximum allowable input power per channel with varying fibre link length at bit rate =10 Gb/s, $M=3$, $N=50$, $\Delta\lambda=1.0$ nm & receiver sensitivity= -14 dBm and BER = 10^{-9} . As mentioned earlier, an increased link length allows less power to launch into fiber input. For example, maximum allowable input power per channel is 6 dBm, 1.5 dBm and -2.5dBm for link length of 25 km, 100km, and 200 km respectively.

Fig.4.25 shows BER variation with optical input power per channel for different values of channel spacing at bit rate 10 Gb/s, $M=3$, receiver sensitivity -14dBm and $L=25$ km. It is shown in the crosstalk analysis that due to combine influence of SRS and XPM, denser wavelength spacing increases crosstalk. So, large channel spacing allows much power to launch into fiber input.

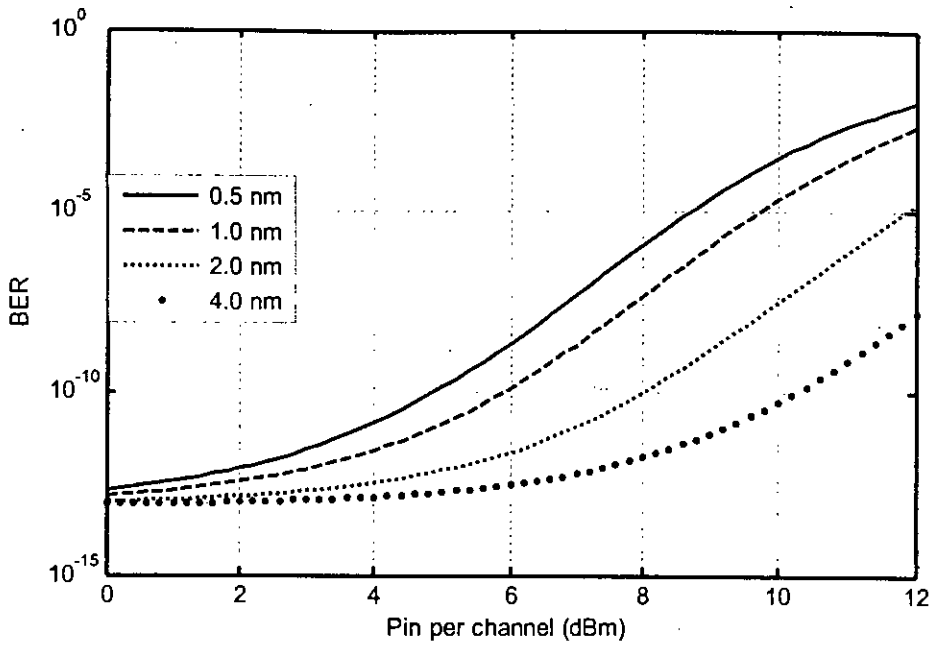


Fig.4.25. BER as a function of optical input power per channel for different channel spacing at bit rate =10 Gb/s, receiver sensitivity = -14dBm, M=3, and L=25km.

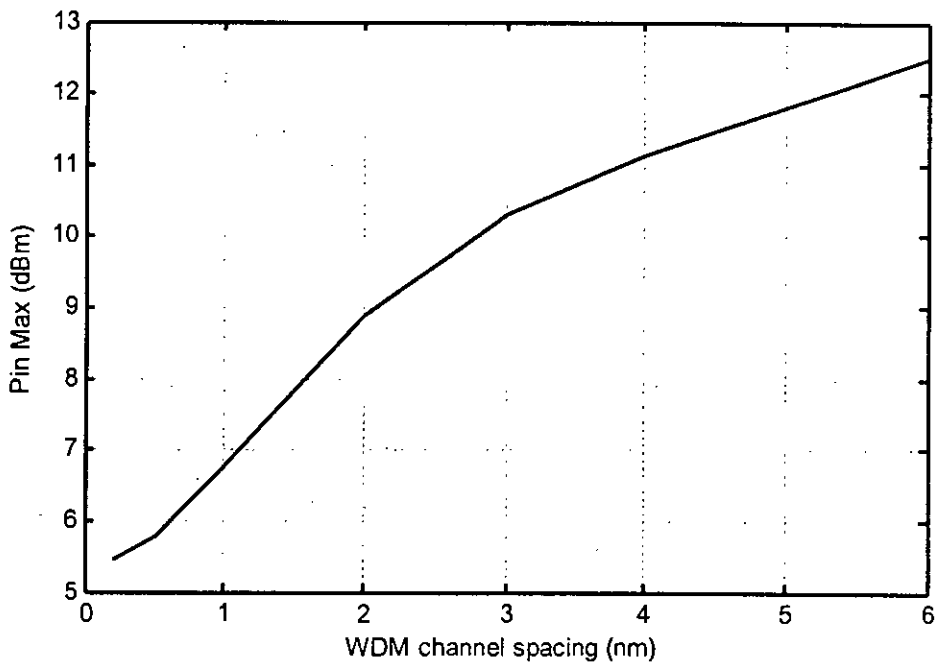


Fig.4.26: Maximum allowable optical input power at BER of 10^{-9} with varying channel spacing at bit rate =10 Gb/s, M=3, N=50, L=25km and receiver sensitivity= -14 dBm.

Effect of channel spacing is further confirmed in Fig.4.26 where maximum allowable input power is plotted as a function of wavelength channel spacing at BER of 10^{-9} , bit rate =10 Gb/s, M=3, N=50, L=25km and receiver sensitivity= -14 dBm. Allowable input power increases to 5.8 dBm to 9 dBm for an increase of channel spacing from 0.5 nm to 2.0 nm.

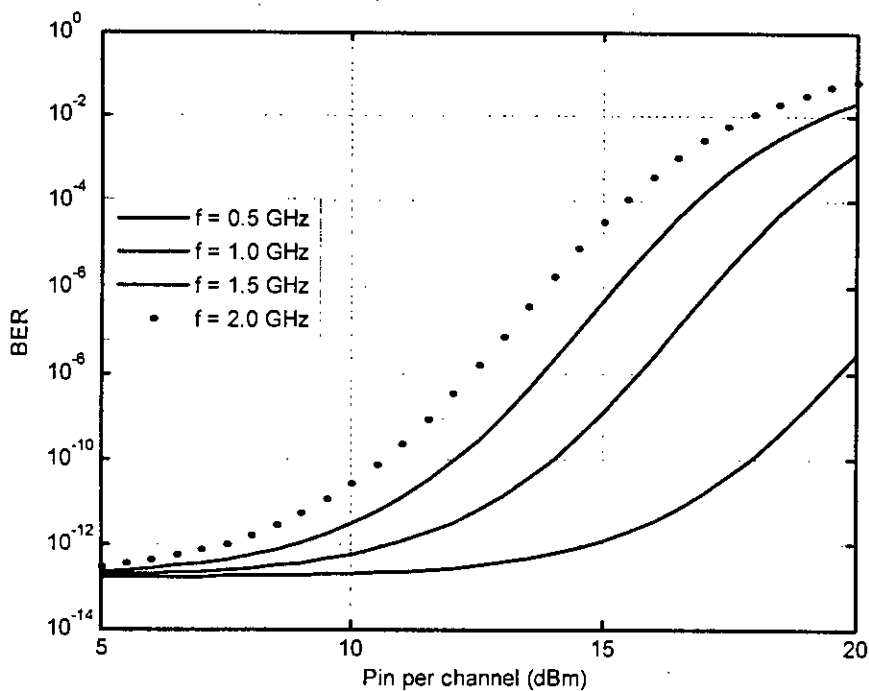


Fig.4.27. BER as a function of optical input power per channel for different modulation frequency at for $\Delta\lambda=1.0$, receiver sen. = -14dBm, M=3, and L=25km.

Fig. 4.27 shows the effect of modulation frequency on BER performance of the system for $\Delta\lambda=1.0$, receiver sen. = -14dBm, M=3, and L=25km. As mentioned earlier, if modulation frequency is increased, crosstalk also increases. Hence BER of the system will also increase.

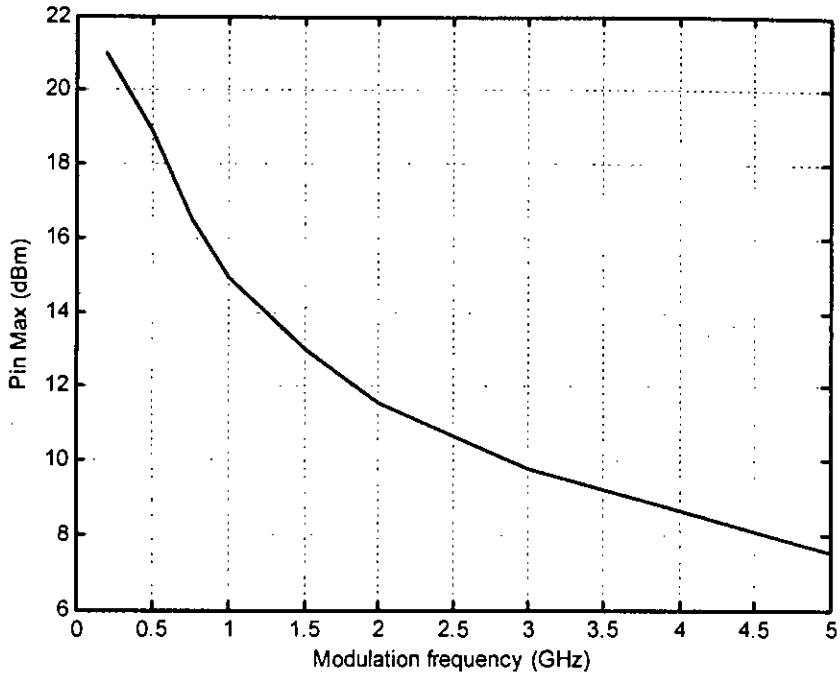


Fig.4.28: Maximum allowable optical input power at BER of 10^{-9} with varying modulation frequency for $L=25$ km, $M=3$, $N=50$, $\Delta\lambda=1.0$ nm & Rx. sen.= -14 dBm.

Fig. 4.28 shows maximum allowable input power per channel with varying modulation frequency at BER of 10^{-9} , $M=3$, $N=50$, $\Delta\lambda=1.0$ nm & receiver sensitivity=-14 dBm. As mentioned earlier, an increased modulation frequency increases crosstalk and allows less power to launch into fiber input. For example, maximum allowable input power per channel is 15 dBm, 11.5 dBm and 9.5 dBm for modulation frequency of 1 GHz, 2 GHz and 3 GHz respectively.

4.6 PERFORMANCE ANALYSIS USING DSF

While using DSF, FWM is the major crosstalk contributing phenomena. In this section performance results are given for DSF considering FWM effect.

Fig.4.29 shows the carrier to noise plus crosstalk ratio with varying receiver sensitivity for different values of optical input power per channel at bit rate 10 Gb/s, $L=25$ km, $\Delta\lambda=0.8$ nm, $M=3$, $N=50$. As mentioned earlier, with increase of input power, crosstalk due to FWM increases as a factor of P_{in}^3 and thus decreasing CNR of the system. For example, with a receiver sensitivity of -15 dBm, for optical input power of -5 dBm, 0 dBm and 3 dBm, CNR are 22 dBm, 16.2 dBm and 9 dBm respectively.

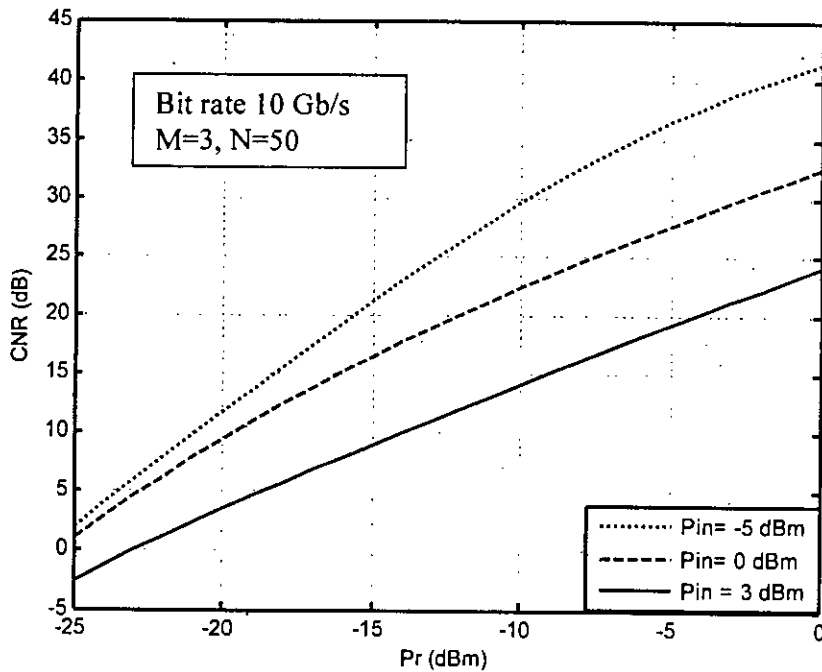


Fig.4.29: CNR of a RF channel with varying received power for different values of input power at bit rate 10 Gb/s, $L=25$ km, $\Delta\lambda=0.8$ nm, $M=3$, $N=50$.

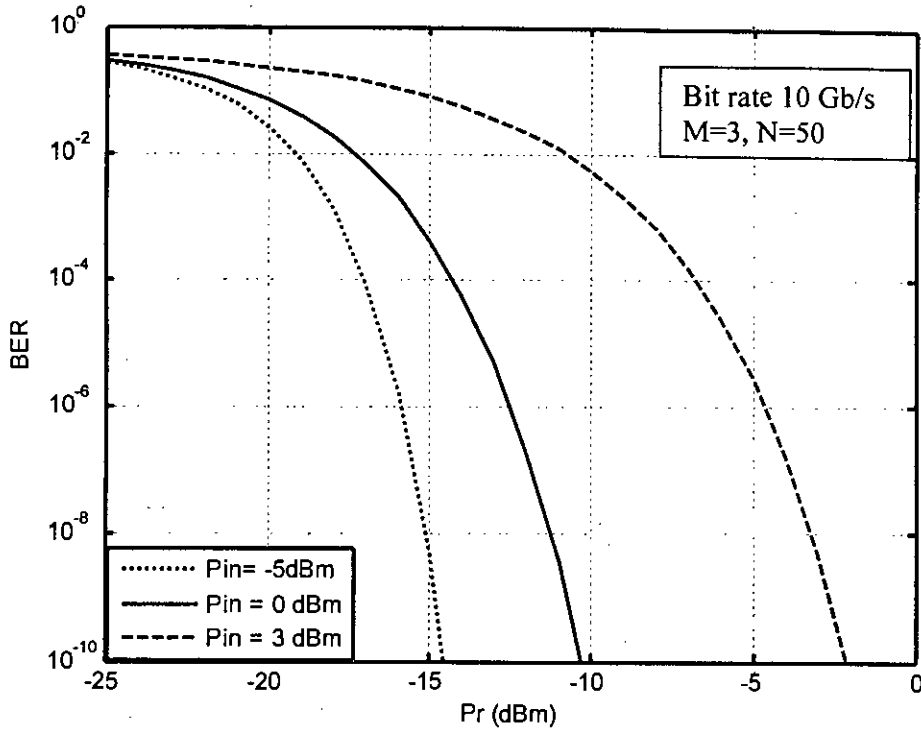


Fig.4.30: BER of a RF channel with varying received power for different values of input power at bit rate 10 Gb/s, $L=25$ km, $\Delta\lambda=0.8$ nm, $M=3$, $N=50$.

BER in presence of FWM crosstalk with varying receiver sensitivity for different optical input power per channel is shown in Fig.4.30 at bit rate 10 Gb/s, $L=25$ km, $\Delta\lambda=0.8$ nm, $M=3$, $N=50$. With increasing input power crosstalk increases and thus a higher receiver sensitivity is required for a given BER. For example, at BER 10^{-9} required receiver sensitivities are -14.75 dBm, -11 dBm and -2.5 dBm for input power of -5 dBm, 0 dBm and 3 dBm respectively.

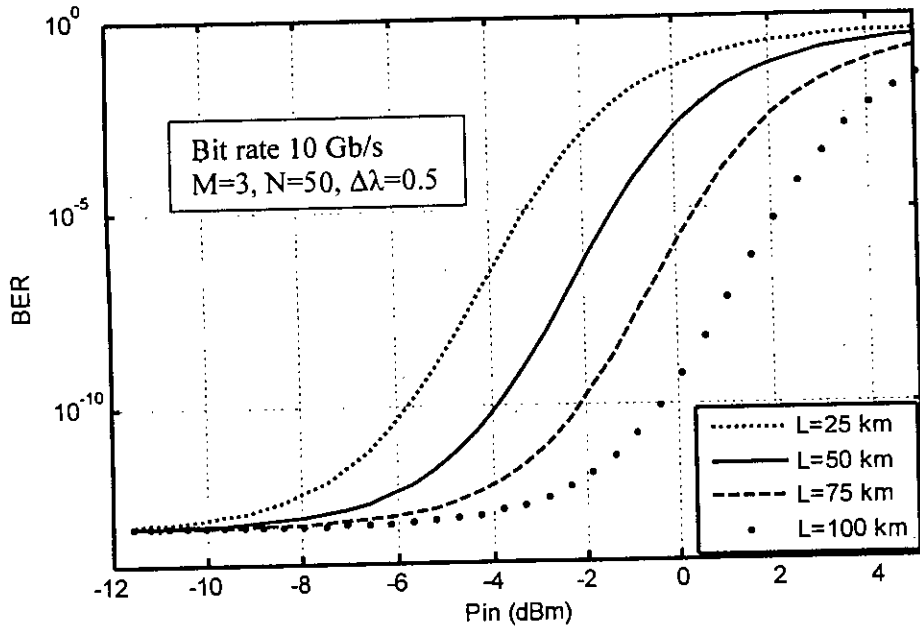


Fig.4.31: BER as a function of optical input power per channel for different link length at bit rate =10Gb/s, $M=3$, $N=50$, $\Delta\lambda=0.5$ nm and receiver sensitivity = -14 dBm.

BER of the system in presence of FWM as a function of optical input power per channel is shown in Fig. 4.31 for a receiver sensitivity of -14 dBm at different fiber link length at bit rate =10Gb/s, $M=3$, $N=50$, $\Delta\lambda=0.5$ nm. It is found that BER increases with increasing input power per channel as FWM crosstalk increases with increasing input power. Again as length increases, FWM generated power decreases for fiber attenuation. Thus long distance system allows launching of large input power per channel.

Fig.4.32 shows the maximum allowable power per channel with varying input power at a BER of 10^{-9} , bit rate =10 Gb/s, $M=3$, $N=50$, $\Delta\lambda=0.5$ nm and receiver sensitivity = -14 dBm. As discussed earlier, long distance system allows launching of large power to fiber input. For example, Maximum allowable power is -4.97 dBm, -3.3 dBm, 0.2 dBm and 7 dBm for link length of 25 km, 50 km, 100 km and 200 km respectively.

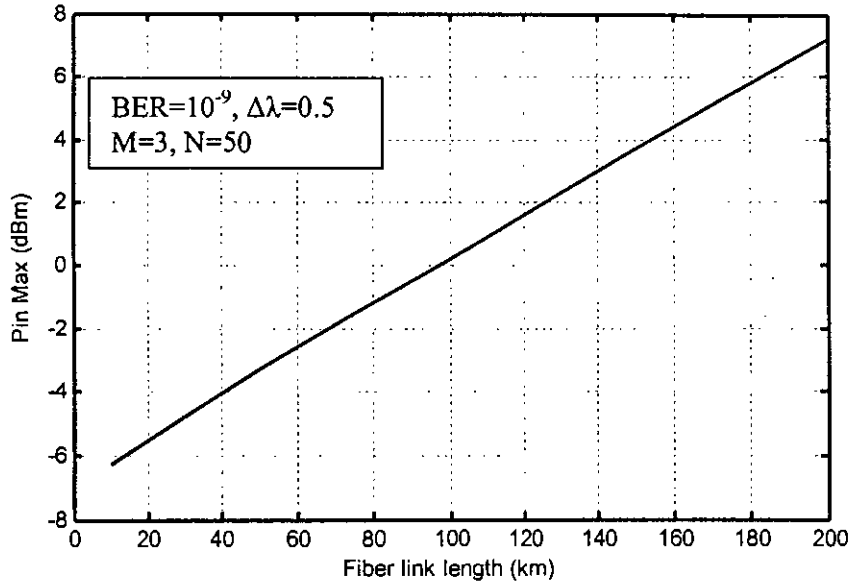


Fig.4.32: Maximum allowable optical input power at BER of 10^{-9} with varying fibre link length for bit rate =10Gb/s, $M=3$, $N=50$, $\Delta\lambda=0.5$ nm & receiver sen. = -14 dBm.

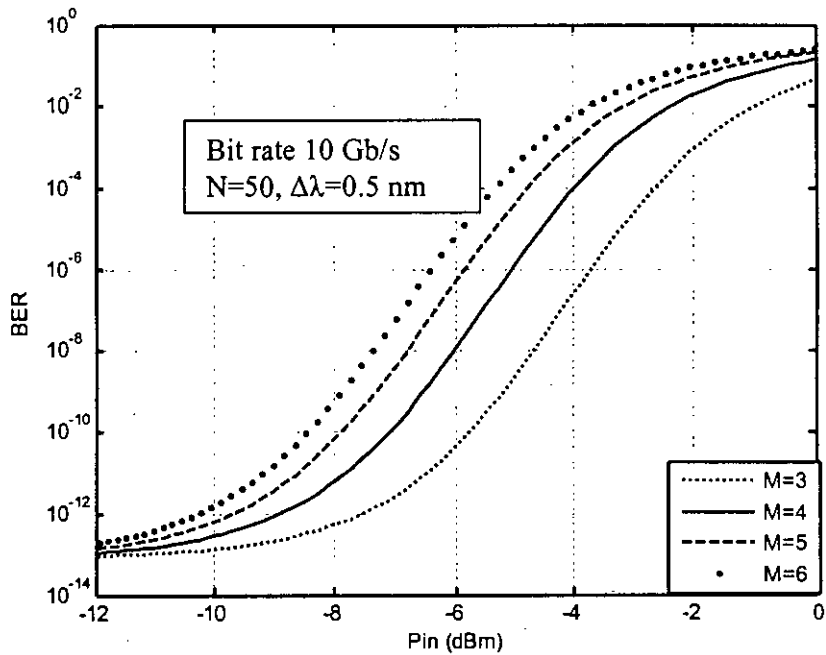


Fig.4.33. BER as a function of optical input power per channel for different number of WDM channel for Bit rate =10Gb/s, receiver sen. = -14dBm, $N=50$, $\Delta\lambda=0.5$ nm, and $L=25$ km.

Fig.4.33 shows BER of the system considering FWM with varying optical input power per channel for different number of WDM channels at bit rate =10Gb/s, $N=50$, $\Delta\lambda=0.5$ nm, $L=25$ km and receiver sensitivity= -14 dBm. While increasing M , as predicted in the theoretical analysis, crosstalk increases and thus allowing less optical power to launch to fiber input. It is further confirmed in Fig. 4.34, where maximum allowable power for a BER of 10^{-9} is shown for different values of M at receiver sensitivity of -14 dBm. As shown in the figure, maximum allowable power per channel decreases to -9.2 dBm from -5.2 dBm while increasing number of WDM channel from 3 to 10.

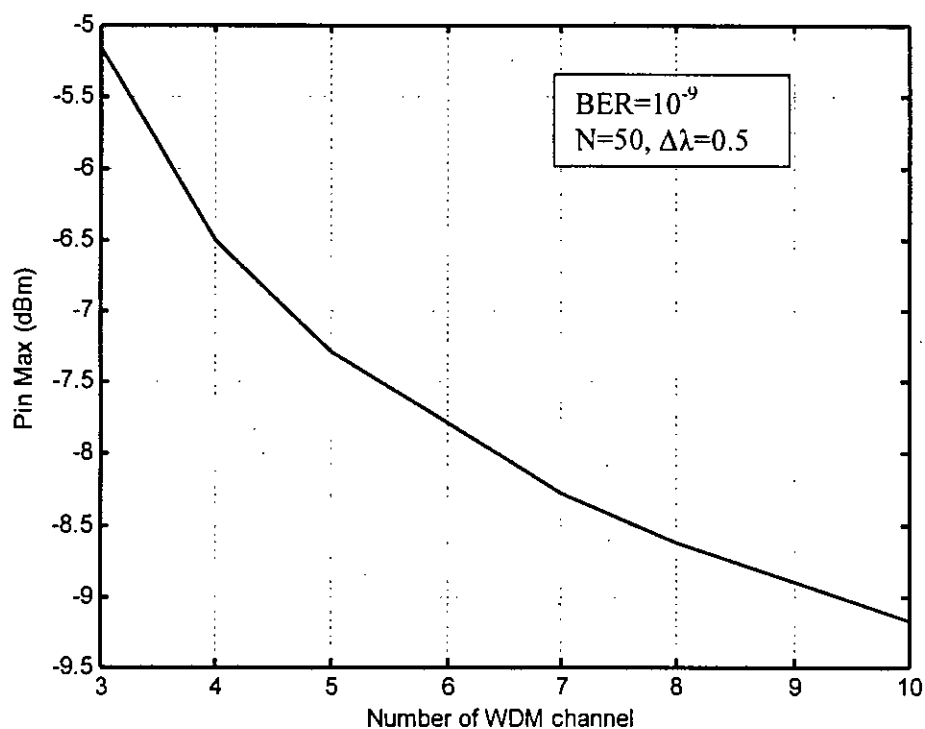


Fig.4.34: Maximum allowable optical input power at BER of 10^{-9} with varying number of WDM channel for Bit rate =10Gb/s, $N=50$, $\Delta\lambda=0.5$ nm, $L=25$ km and receiver sensitivity= -14 dBm.

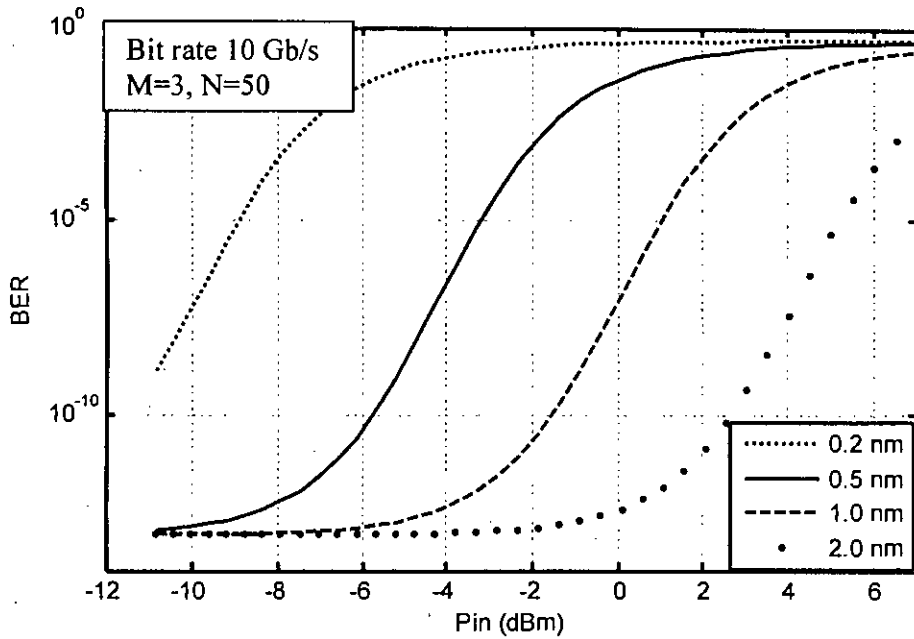


Fig.4.35. BER as a function of optical input power per channel for different channel spacing at bit rate =10 Gb/s, receiver sensitivity = -14dBm, M=3, N=50 and L=25 km.

FWM crosstalk increases largely while decreasing channel spacing of WDM channel as FWM phase mismatch efficiency is at very high value at channel spacing below 0.5 nm for a dispersion shifted fibre. Thus while increasing channel spacing, more power is allowed to launch into fibre input for a particular BER as shown in Fig.4.35.

Maximum allowable input power per channel as a function of channel spacing is shown in Fig 4.36 at bit rate =10 Gb/s, M=3, N=50, L=25km and receiver sensitivity= -14 dBm. It is found from the figure that for decreasing channel spacing from 1 nm to 0.2 nm maximum allowable power decreases from -1 dBm to -11 dBm.

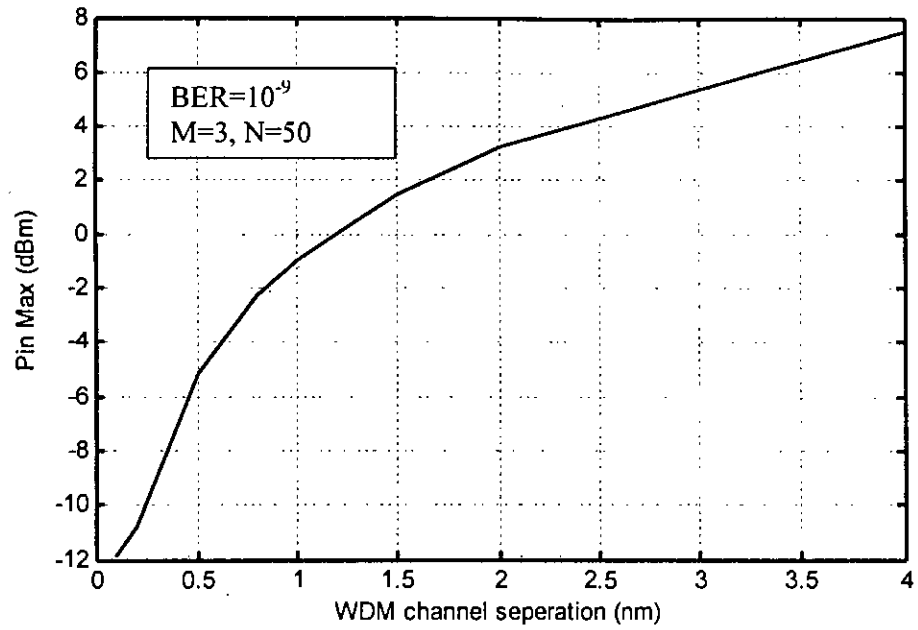


Fig.4.36: Maximum allowable optical input power at BER of 10^{-9} with varying channel spacing for Bit rate =10 Gb/s, $M=3$, $N=50$, $L=25\text{km}$ and receiver sensitivity= -14 dBm.

So, we can conclude that allowable optical input power per WDM channel decreases with denser WDM channel spacing or larger number of M and N or decreasing fibre link length.

CHAPTER-5

CONCLUSION AND FUTURE WORK

1.1 CONCLUSION

A detailed theoretical analysis is carried out to evaluate the impact of fiber nonlinear effects viz. cross phase modulation (XPM), stimulated Raman scattering (SRS) and four-wave mixing (FWM) on the performance of a subcarrier multiplexed WDM transmission system. The subcarrier modulation is considered as MSK with optical intensity modulation and in the receiver side direct detection is used while coherent detection is used for subcarrier. Performance result is evaluated at a bit rate of 10 Gb/s for both standard SMF and DSF at a wavelength of 1550 nm for a several set of system parameters.

While analyzing effect of XPM induced crosstalk on SCM-WDM system, it is found central WDM channel is mostly affected by XPM crosstalk. It is also found that XPM crosstalk is dominant in standard SMF than DSF. For example, for P_{in} per channel 10 dBm, $f=1$ GHz, $\Delta\lambda = 1$ nm & $L=25$ km crosstalk in SMF is -15 dBm while for DSF -35 dBm. It is also found that with increasing fiber link length, XPM crosstalk increases due to more interactions among the channels. It is further noticed that, XPM crosstalk is dominant with dense wavelength separation and large modulation frequency.

A contrary characteristic is found for SRS induced crosstalk. SRS crosstalk is dominant at large channel separation (up to a limit) and lower modulation frequency. Again, highest wavelength channel is mostly affected SRS, unlike XPM where it is central channel. So, while investigating combined influence of SRS & XPM induced crosstalk, it is an interesting issue to find the worst channel – central channel or highest wavelength channel. Computed results show that for a three channel WDM system, 1GHz modulation frequency, 1 nm WDM channel spacing and 10 dBm optical power per channel, the highest wavelength channel suffers mostly by crosstalk up to 40 km and central channel beyond this length.

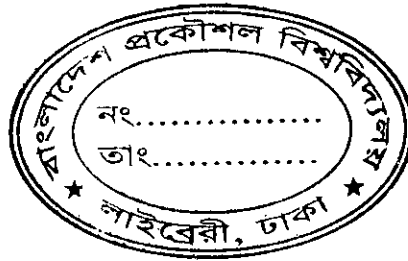
FWM crosstalk is dominant in DSF than normal SMF. For example, for $M=3$, $N=50$, $P_{in}=0$ dBm, $L=25$, bit rate 10 Gb/s and $\Delta\lambda = 0.5$ nm, FWM crosstalk is -52.5 dBm for SMF and -32 dBm for DSF. FWM crosstalk level is plotted for a set of system parameters such as channel separation, number of WDM channels, number of subcarriers per channel etc. It is found that FWM crosstalk is larger in denser wavelength separation. It is further noticed that FWM crosstalk increases with increasing number of subcarriers and largely with increasing number of wavelength channel.

To determine BER performance considering fiber nonlinear effects, FWM is considered for DSF and SRS & XPM for SMF. To investigate the effect of FWM, receiver sensitivity is kept constant while input power is varied. The results show that there is a significant amount of increase in the system BER with increase in input power per channel, P_{in} , due to increased FWM effect. However, at longer fiber length, FWM power is less due to fiber loss which results in lower BER for same P_{in} . While increasing number of WDM channels, crosstalk due to FWM increases and thus allowing less optical power to launch into fiber input. For example, for bit rate =10Gb/s, $N=50$, $\Delta\lambda=0.5$ nm, $L=25$ km and receiver sensitivity= -14 dBm maximum allowable power at a BER of 10^{-9} decreases to -9.2 dBm from -5.2 dBm while increasing number of WDM channel from 3 to 10. Increasing channel spacing, crosstalk decreases, thus increasing maximum allowable power. For example, for $\Delta\lambda=0.5$ nm P_{in} max is -5 dBm whereas it increases to 3.5 dBm for $\Delta\lambda=2.0$ nm. For SMF, it is found that as combined crosstalk of SRS and XPM increase with fiber link length, long length system limiting the maximum allowable input power to fiber. For example, at bit rate =10 Gb/s, $M=3$, $\Delta\lambda=1.0$ nm, receiver sensitivity= -14 dBm and BER = 10^{-9} maximum allowable input power per channel is 6 dBm, 1.5 dBm and -2.5dBm for link length of 25 km, 100km, and 200 km respectively. It is shown in the crosstalk analysis that due to combine influence of SRS and XPM, denser wavelength spacing increases crosstalk, thus maximum allowable power increases with increasing channel spacing.

1.2 FUTURE WORK

Future work can be carried out to investigate the effect of self phase modulation (SPM), Stimulated Brilluin Scattering (SBS) and polarization mode dispersion (PMD) on SCM-WDM system. Two nonlinear terms generated in MZ modulator is composite second order (CSO) and composite triple beat (CTB). Future study in CSO and CTB is suggested. Analysis can also be carried out for other modulation format for subcarrier modulation such as AM-VSB, QPSK, M-ary QAM etc.

Future work in this area can also be carried out for the experimental validation of the theoretical results and to determine the optimum system parameters for reliable system performance.



REFERENCES

- [1] Winston I. Way, "Subcarrier Multiplexed Lightwave System Design Considerations for Subscriber Loop Applications," *J. Lightwave Technol.*, vol. 7, pp. 1989-2002, Nov. 1989.
- [2] Charles N. Lo, "A Hybrid Lightwave Transmission System for Subcarrier Multiplexed Video and Digital B-ISDN Services in the Local Loop," *J. Lightwave Technol.*, vol. 7, pp. 1839-1849, Nov. 1989.
- [3] Robert Olshansky, Vincent A. Lanzisera, Paul M. Hill, "Subcarrier Multiplexed Lightwave Systems for Broad-Band Distribution," *J. Lightwave Technol.*, vol. 7, no.9, pp. 1329-1333, Sep. 1989.
- [4] Paul M. Hill, Robert Oalshansky, "A 20-Channel Optical Communication System Using Subcarrier Multiplexing for the Transmission of Digital Video Signals," *J. Lightwave Technol.*, vol. 8, no.4, pp. 554-561, April. 1990.
- [5] Yang-Han Lee, Jingshown Wu, and Ben-Wai Tsao, "The Impact of laser Phase Noise on the Coherent Subcarrier Multiplexing System," *J. Lightwave Technol.*, vol. 9, no.3, pp. 347-356, Mar. 1991.
- [6] Robert Olshansky, "Optimal Design of Subcarrier Multiplexed Lightwave Systems Employing Linearized External Modulators," *J. Lightwave Technol.*, vol. 10, no.3, pp. 378-383, Mar. 1992.
- [7] Paul M. Hill, and Robert Olshansky, "Multigigabit Subcarrier Multiplexed Coherent Lightwave System," *J. Lightwave Technol.*, vol. 10, no.11, pp. 1656-1665, Nov. 1992.
- [8] D. Tang, P. Hill and R. Olshansky, "Sensitivity Improvement of a 2 Gb/s Quardature Phase Shift Keyed Subcarrier Multiplexed System by Use of an Optical Preampfier," *Photon. Techol. Lett.*, vol. 2, pp. 282 - 284, 1990.

- [9] Isam M. I. Habbab, and Adel A. M. Saleh, "Fundamental Limitations in EDFA-Based Subcarrier-Multiplexed AM-VSB CATV Systems," *J. Lightwave Technol.*, vol. 11, no.1, pp. 42-49, Jan. 1993.
- [10] Robert Olshansky, Vincent A. Lanzisera, Shing-Fong Su, Richard Gross, Albert M. Forcucci, and A. Hugh Oakes, "Subcarrier Multiplexed Broad-Band Service Network: A Flexible Platform for Broad-Band Subscriber Services," *J. Lightwave Technol.*, vol. 11, no.1, pp. 60-70, Jan. 1993.
- [11] Kamal E. Alameh and Robert A. Minasian, "Optimization of Fiber Amplifier SCM Lightwave Video Systems Using Direct and External Modulation," *J. Lightwave Technol.*, vol. 11, no.1, pp. 76-82, Jan. 1993.
- [12] George J. Meslener, "Mode-Partition Noise in Microwave Subcarrier Transmission Systems," *J. Lightwave Technol.*, vol. 12, no.1, pp. 118 - 127, Jan. 1994.
- [13] Koji Kikushima, KO-ichi Suto, Hisao Yoshinaga, and Etsugo Yoneda, "Polarization Dependent Distortion in AM-SCM Video Transmission Systems," *J. Lightwave Technol.*, vol. 12, no.4, pp. 118 - 127, Apr. 1994.
- [14] Xiaolin Lu, C. B. Su, R. B. Lauer, G. J. Meslener, and L. W. Ulbricht, "Analysis of Relative Intensity Noise in Semiconductor Lasers and Its Effect on Subcarrier Multiplexed Lightwave Systems," *J. Lightwave Technol.*, vol. 12, no.7, pp. 1159 - 1168, July 1992.
- [15] Ming-Kang Liu and Panayiotis C. Modestou, "Multilevel Signaling and Pulse Shaping for Spectrum Efficiency in Subcarrier Multiplexing Transmission," *J. Lightwave Technol.*, vol. 12, no.7, pp. 1239 - 1246, July 1994.

- [16] Farideh Khaleghi, and Mohsen Kavehrad, "A Subcarrier Multiplexed CDM Optical Local Area Network, Theory and Experiment," *J. Lightwave Technol.*, vol. 43, no.1, pp. 95 - 108, Jan. 1995.
- [17] Mohammad M. Banat, and Mohsen Kavehrad, "Reduction of Optical Beat Interference in SCM/WDMA Networks Using Pseudorandom Phase Modulation," *J. Lightwave Technol.*, vol. 12, no.10, pp. 95 - 108, Oct. 1994
- [18] Attilio J. Rainal, "Limiting Distortion of CATV Lasers," *J. Lightwave Technol.*, vol. 14, no.3, pp. 474- 480, Mar. 1996.
- [19] Surachet Kanprachar and Ira Jacobs," Diversity Coding for Subcarrier Multiplexing on Multimode Fibers," *IEEE Trans. On Communication*, vol. 51, no.9, pp. 1546 - 1554, Sep. 2003.
- [20] R. Hui, B. Zhu, R. Huang, C. Allen, K. Demarest, and D. Richards, "10-Gb/s SCM Fiber System using Optical SSB Modulation," *J. Lightwave Technol.*, vol. 13, no. 8, pp. 896- 899, Aug. 2001.
- [21] Rongqing Hui, Benyuan Zhu, Renxiang Huang, Christopher T. Allen, Kenneth R. Demarest, and Douglas Richards," Subcarrier Multiplexing for High-Speed Optical Transmission," *J. Lightwave Technol.*, vol. 20, no.3, pp. 417- 428, Mar. 2002.
- [22] Z. Wang, A. Li, C.J. Mahon, G. Jacobsen and F. Bodtker, "Performance limitation imposed by stimulated Raman scattering in optical WDM SCM video distribution system," *IEEE photon. Technol. Lett.*, vol. 7, pp. 1492 - 1494, Dec. 1995.
- [23] Z. Wang, E. Bodtker, and G. Jacobsen, "Effect of cross phase modulation in wavelength multiplexed-SCM video transmission systems," *Electron. Lett.*, vol. 31, pp. 1591 - 1592, Aug. 1995.

- [24] M.R. Phillips and D. M. Ott, "Crosstalk due to optical fibre nonlinearities in WDM CATV lightwave system," *J. Lightwave Technol.*, vol. 17, pp. 1782-1792, Oct. 1999.
- [25] F.S. Yang, M.E. Marhic and L.G. Kazovsky, "Nonlinear crosstalk and two countermeasures in SCM-WDM Optical communication system," *J. Lightwave Technol.*, vol. 18, pp. 512-520, Apr. 1999.
- [26] S.L. Woodward and M.R. Phillips, "Optimizing Subcarrier - Multiplexed WDM transmission link," *J. Lightwave Technol.*, vol. 12, pp. 773-778, Mar. 2004.
- [27] W. H. Chen and Winston I. Way, "Multichannel Single-Sideband SCM/DWDM Transmission Systems," *J. Lightwave Technol.*, vol. 22, no.7 pp. 1679-1694, July 2004.
- [28] V Kumar, A K Sharma and A R Agarwal, "Non linear crosstalk in Dispersive SCM/WDM Optical communication System," *IE(I) Journal ET* vol. 85, pp. 42-44, Jan. 2005.
- [29] S. Subramaniam, F. M. Abbou, H. T. Chuah and K. D. Dambul, "Performance Evaluation of SCM-WDM Microcellular Communication System in Presence of XPM," *IEICE Electronic Express*, vol. 2, no. 6, pp. 192-197, Mar. 2005.
- [30] K. Inoue, "Four-Wave Mixing in an Optical Fiber in the Zero-Dispersion Wavelength Region," *J. Lightwave Technol.*, vol. 10, pp. 1553-1561, Nov. 1992.
- [31] Kyo Inoue, "Experimental Study on Channel Crosstalk Due to Fiber Four-Wave Mixing Around the Zero-Dispersion Wavelength," *J. Lightwave Technol.*, vol. 12, no. 6 pp. 1023-1029, June 1994.

- [32] K. Inoue, K. Nakanishi, K. Oda and H. Toba, "Crosstalk and Power Penalty in due to Fiber Four Wave Mixing in Multichannel Transmissions," *J. Lightwave Technol.*, vol. 12, no. 8 pp. 1423 - 1440, Aug. 1996.
- [33] Wolfgang Zeiler, Fabrizio Di Pasquale, Polina Bayvel and John E. Midwinter "Modeling of Four-Wave Mixing and Gain Peaking in Amplified WDM Optical Communication Systems and Networks," *J. Lightwave Technol.*, vol. 14, no. 6 pp. 1933-1940, June 1996.
- [34] Michael Eiselt "Limits on WDM Systems Due to Four-Wave Mixing: A Statistical Approach," *J. Lightwave Technol.*, vol. 17, no. 11 pp. 2261 - 2268, Aug. 1999.
- [35] S. Song, C.T. Allen and R.Hui, "Intensity - dependent phase matching effects on four-wave mixing in optical fibers," *J. Lightwave Technol.*, vol. 17, pp. 2285-2290, Nov. 1999.
- [36] Bo Xu and Maïté Brandt-Pearce "Comparison of FWM- and XPM-Induced Crosstalk Using the Volterra Series Transfer Function Method," *J. Lightwave Technol.*, vol. 21, no. 1, pp. 40 - 54, Jan. 2003.
- [37] Mingchia Wu and Winston I. Way "Fiber Nonlinearity Limitations in Ultra-Dense WDM Systems," *J. Lightwave Technol.*, vol. 22, no. 6, pp. 1483 - 1497, July 2004.
- [38] Shiva Kumar "Analysis of Degenerate Four-Wave-Mixing Noise in Return-to-Zero Optical Transmission Systems Including Walk-Off," *J. Lightwave Technol.*, vol. 23, no. 1 pp. 310 - 321, Jan. 2005.
- [39] I.Neokosmidis, T. Kamalakis, A. Chipouras, and T. Sphicopoulos, "New Techniques for the Suppression of the Four-Wave Mixing-Induced Distortion in Nonzero Dispersion Fiber WDM Systems," *J. Lightwave Technol.*, vol. 23, no. 3, pp. 1137 - 1145, Mar. 2005.

- [40] Rongqing Hui, Kenneth R. Demarest, and Christopher T. Allen "Cross-Phase Modulation in Multispan WDM Optical Fiber Systems," *J. Lightwave Technol.*, vol. 17, no. 6, pp. 1018 - 1027, June 1999.
- [41] Surachet Kanprachar, "Modeling, Analysis, and Design of Subcarrier Multiplexing on Multimode Fiber," Ph.D. thesis, Virginia Polytechnic Instituted and State University, Mar. 2003. ✓
- [42] Renxiang Huang, "Simulation and Experimental Study of SCM/WDM Optical Systems," M.Sc. thesis, University of Kansas, May 2003. ✓
- [43] S. Subramaniam, "Performance Evaluation of an SCM/WDM Fibre Microcellular Mobile Communication System Based on IM/DD," M.Sc. thesis, Multimedia University, Aug. 2004. ✓
- [44] Anthony Leung, "Performance Analysis of SCM Optical Transmission Link for Fiber-to-the-Home," M.Sc. thesis, University of Kansas, 2004. ✓
- [45] G. P. Agarwal, *Nonlinear Fibre Optics*, 2nd ed. New York, 1995.
- [46] Harry J. R. Dutton, *Understanding Optical Communications*, IBM Corporation, International Technical Support Organization, 1998
- [47] J. H. Franz and V. K. Jain *Optical Communications Components and Systems*, Narosa Publishing House, India, 2001
- [48] G. P. Agarwal *Fiber-Optic Communication System*, 3rd ed. John Wiley & Sons Publication, New York, 2002.
- [49] Simon Haykin, *Digital Communications*, John Wiley & Sons Publication, New York, 2003.
- [50] John M. Senior, *Optical Fiber Communications – principle and Practice* 2nd ed. Prentice Hall of India, 2004.

